Capability of CORDEX RCMs in simulating extreme rainfall events over South Africa

Master's dissertation

by

Sabina Abba Omar (ABBSAB001)

Presented towards the degree of Master's of Science

in Environmental and Geographical Science

University of Cape Town

February 2014

Supervisor: Dr. Babatunde J. Abiodun

Declaration

1. I know that plagiarism is wrong. Plagiarism is to use another's work and pretend that it is one's own.
2. I have used the Harvard convention for citation and referencing. Each contribution and quotation in this dissertation from the works of other people has been attributed and has been cited and referenced.
3. This dissertation is my own work.
4. I have not allowed, and will not allow, anyone to copy this work with the intention of passing it off as his or her own.

17 February 2014

Sabina Abba Omar

Dedication

To my mother,

Therese Marie Raubenheimer

Abstract

In South Africa, extreme rainfall events often lead to widespread destruction, damage infrastructure, displace communities, strain water management and even destroy lives. Past studies have shown that reliable predictions of extreme rainfall events from regional climate models (RCMs) could help reduce the impact of these events. The present study evaluates the ability of nine RCMs in simulating extreme rainfall events over South Africa, focusing on the Western Cape (WC) and east coast (EC) areas. This study defines an extreme rainfall over a location as rainfall that is equal to or above the 95th percentile of the rainfall distribution at that location, and defines widespread extreme rainfall events (WEREs) over an area as events during which more than 50% of the grid-points in the area experience extreme rainfall. The 95th percentile threshold values were calculated over 11 years (1998-2008) of South Africa's daily rainfall data from the nine RCMs (CCLM, REMO, PRECIS, CRCM5, ARPEGE, REGCM3, WRF, RACMO and RCA35), which participated in the Coordinated Regional Climate Downscaling Experiment (CORDEX) and used ERA-Interim (ERAINT) as their boundary forcing. The simulations were compared to two observation datasets (TRMM and GPCP), and to ERAINT rainfall data to understand whether these RCMs improve on the results from ERAINT. A self organizing map (SOM) was used to characterize WEREs identified in all the datasets into archetypal groups, and ERAINT data is used to describe the underlying circulations for each archetypal rainfall pattern. The number of WEREs mapped to each rainfall pattern for each dataset allows us to get an idea of whether certain RCMs are more likely to simulate certain rainfall patterns.

The results show that RCA35, REMO and WRF seem to be the best at simulating the 95th percentile threshold values over the whole of South Africa, but CCLM performs best in simulating the threshold values over the WC, while PRECIS performs best in simulating the threshold values over the EC. However, downscaling ERAINT with CCLM produces fewer WEREs, whereas downscaling ERAINT with PRECIS produces a higher number of WEREs simulated over both areas (WC and EC). The SOMs identifies five major patterns of WEREs over these areas. The first pattern (TRW) links a WERE in WC or EC with tropical activities, producing a tropical

temperate through that is truncated at the coast. The second pattern (MLW) links a WERE in WC or EC with mid-latitude rainfall activities. The third pattern (ISW) produces an isolated WERE over each area. The fourth pattern (ACW), which is unique to WC, links a WERE in WC with rainfall activities over the Agulhas current. The fifth pattern (TMW), which is unique to EC, links WEREs in EC with both tropical and mid-latitude rainfall activities, hence producing elongated TTTs. PRECIS has the tendency to overestimate the frequency of TRW over both the EC and WC whereas, WRF only shows this tendency over the EC. ARPEGE simulations overestimate the frequency of ISW over the EC area, while WRF and CRCM5 underestimate it over WC. All RCMs give reasonable simulations of MLW frequency over EC, but most of the RCMs overestimate the frequency over WC.

Acknowledgements

There a number of people that I would like to acknowledge for their support. Firstly and most importantly, I would like to thank my supervisor, Dr. Babatunde Abiodun, for his guidance and support throughout the thesis process. I want to thank him for always motivating me - after a meeting with him the work always seemed less daunting and more fun. I also want to thank him for providing the inspiration and knowledge for this project.

I am also grateful for the financial support provided by the National Research Fund and the University of Cape Town, without which I would not have been able to complete this degree. I would like to acknowledge the various institutions that provided data for my project: the Climate System Analysis Group (CSAG), and the various climate modeling groups who provided the RCM data, TRMM, GPCP and the European Centre for Medium-Range Weather Forecasts for the ERA-Interim data (ERAINT). I would like to thank CSAG for giving me access to their high performance computing facilities and to Philip Mukwenha for providing technical support.

To my fellow graduate students in the department, thanks for the shared knowledge, memories and frustrations. Special thanks to Evan Blake, Myra Naik, Stefaan Conradie, Tope Egbebiyi, Nadia du Plessis, Julio Araujo thanks for the many wonderful chats, your intellectual input, the editing and encouragement – knowing that you would be in the office made it so much easier to come to campus and work.

I cannot forget to thank my friends and family. To Penny Garrod and Helen Mc Glead thanks for not disowning. To my flat mate and friend, Megan Stevens- thanks for being sweet and supportive. To Ian Barber, for always being there for me. To my stepdad, Noel Carr thanks for all the good advice. To my brother, Thomas Carr thanks for the love and the laughs. To my father, Mahomed Saleh Abba Omar, thanks for the editing and for the support during the Brussels conference, you made the trip special. To my grandmother, Rita Raubenheimer-thank you for reading and editing my thesis as well as the many chats of encouragement. Lastly to my mother, well words cannot say how grateful I am to you for everything. Without you, I would never be where I am today-thank you!

List of figures

List of tables

List of abbreviations

- CAPE: Convective Available Potential Energy
- CORDEX: Coordinated Regional Climate Downscaling Experiment
- CSAG: Climate System Analysis Group
- EC: east coast region of South Africa, specifically referring to one of the focus regions of this study
- ERAINT: ERA-Interim
- GCM: Global Climate Model
- GEV: Generalized Extreme Value
- GP: Generalized Pareto
- IPCC: Intergovernmental Panel for Climate Change
- ITCZ: Inter-Tropical Convergence Zone
- MFC: Moisture Flux Convergence
- MFD: Moisture Flux Divergence
- RCM : Regional Climate Model
- SAA: South Atlantic Anticyclone
- SAWS: South African Weather Service
- SIA: South Indian Anticyclone
- SOM: self organizing map
- SSTs: sea surface temperatures
- TTT: Tropical Temperate Trough
- WC: Western Cape Province of South Africa, specifically referring to one of the focus regions of this study
- WERE: widespread extreme rainfall event

Table of contents

Chapter 1: Introduction

1.1 What is an extreme rainfall event?

Extreme events can be defined in many different ways. However, there are three predominant ways of defining these events. The first defines an extreme event as extreme if it is higher than a predefined threshold value. The second uses return intervals associated with a specific magnitude to indicate the rarity of the event. The third defines an extreme event as that which lies above a specific threshold percentile of the variables distribution. Nevertheless, The International Panel for Climate Change (IPCC, 2001) defines an extreme weather event as

"an event that is rare within its statistical reference distribution at a particular place. Definitions of 'rare' vary, but an extreme weather event would normally be as rare as, or rarer than, the 10th or 90th percentile. By definition, the characteristics of what is called extreme weather may vary from place to place."

Hence, in this study, we shall define an extreme rainfall event as a rainfall event in which the daily rainfall value is equal to or above the 95th percentile of the daily rainfall distribution.

1.2 South African rainfall characteristics

1.2.1 The topography and rainfall pattern in South Africa

South Africa is the southernmost country of Africa. To the west of South Africa lies the Atlantic Ocean and to the south and south east lies the Indian Ocean. The warm Agulhas Current flows along the south east coast and south coast of South Africa, whereas the relatively cooler Benguela Current flows along the west coast. These two currents contribute to the general spatial pattern of rainfall over South Africa—rainfall decreases as you move west from the east coast over the plateau (Sen Roy & Rouault, 2013). This does not hold true for the southern and far south western coastal areas, due to the higher seaward sloping mountainous regions which help to induce more rainfall over the region (Taljaard, 1996). The plateau in the interior rises to about 1500m above sea level (Figure

1.1). The escarpment on the east coast, which includes the Drakensberg Mountains of KwaZulu-Natal, ranges from 1800 to 3000m above sea level over Lesotho (Taljaard, 1996).

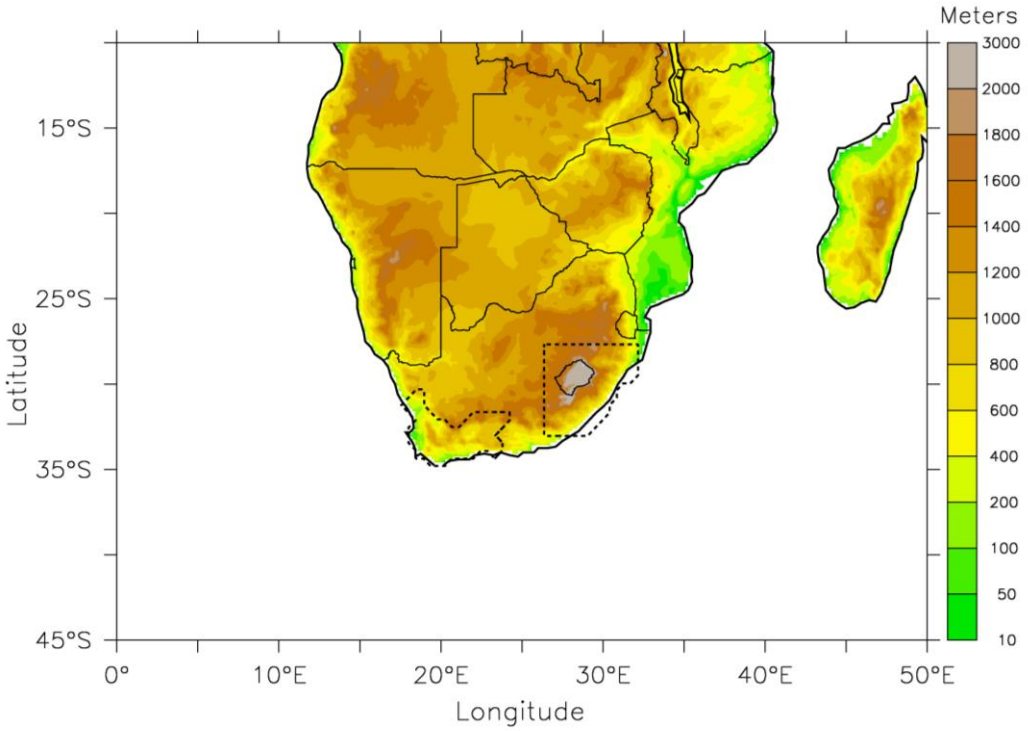

Figure 1.1: The study domain, showing the Southern African topography (shaded), and the Western Cape area(dashed, left) and East Coast area (dashed, right)

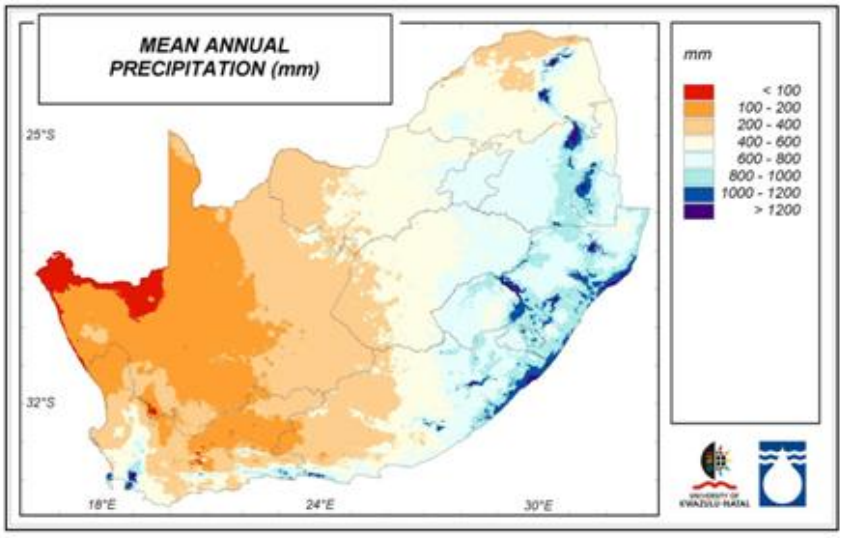

Figure 1.2: The spatial distribution of annual precipitation over South Africa (source: Davis, 2011)

The annual rainfall along the east coast can be greater than 1000mm. The annual rainfall over most of the interior is about 200 to 400mm and over the north-west coast, rainfall can decrease to below 200mm (Figure 1.2). Most of South Africa receives more than half of its rainfall during summer, whereas 12% of the country shows higher rainfall in winter and the south coast receives rainfall during all seasons (Taljaard, 1996). The winter rainfall regions are mainly contained in the Western Cape Province (Taljaard, 1996). While the east coast is a summer rainfall area, it receives more rainfall during winter than further into the interior (Taljaard, 1996).

1.2.2 Synoptic systems that induce rainfall over South Africa

Rainfall can be generated by either, or a combination of, convective processes, cyclonic disturbances or steep topography. The rainfall over the Western Cape generally starts due to the cyclonic disturbances caused by mid latitude cyclones and is aided by the topography of the region, as north westerly winds caused by frontal systems reach the mountain ranges near the south west coast (Taljaard, 1996). This rainfall then continues as instability is experienced during and after the cold front has passed. Over the interior rainfall is dominated by convective processes, whereas, over the east and south coast rainfall due to steep topography and mid-tropospheric divergence, caused by troughs or cut-off lows, dominate (Taljaard, 1996). This makes it clear how rainfall over South Africa can vary over different regions in terms of the intensity and underlying processes. Therefore studies of extreme rainfall events over South Africa will benefit by looking at these different areas rather than the country as a whole.

1.2.2.1 Summer rainfall synoptic systems over South Africa

South Africa's weather is influenced by tropical, subtropical and temperate synoptic systems (Taljaard, 1996). The subtropical anticyclones, namely, the South Atlantic Anticyclone (SAA), the South Indian Anticyclone (SIA) and the continental high, are the dominant features over South Africa (Dyson & van Heerden, 2002; Tyson & Preston-Whyte, 2000; Taljaard, 1996). During summer the SAA and SIA lie on either side of the continent with the SAA ridging south and eastward where it breaks off and is occluded into the SIA. During this time the

Inter-Tropical Convergence Zone (ITCZ) along with the tropical easterlies lie further south, than during winter, which allows the regions of South Africa to be influenced by tropical features, such as tropical cyclones, tropical lows and easterly waves (Tyson and Preston-Whyte, 2000).

Rainfall over South Africa during summer is mainly caused by westerly troughs, the southerly extension of tropical lows and troughs, tropical cyclones, ridging highs and blocking highs (Taljaard, 1996). When the ITCZ is extended further south so are the easterly waves and their associated tropical troughs and lows (Tyson & Preston-Whyte, 2000; Taljaard, 1996). The troughs associated with these waves result in convergence at the surface, occurring to the east of the trough, and divergence above as the troughs are generally replaced by anticyclonic circulation at 500hPa or higher. This results in strong uplift which can cause rainfall even in stable conditions. Generally higher rainfall is seen when these features occur in association with northerly winds. Convergence is also seen to the east of tropical lows but divergence is seen higher up in the atmosphere compared to the troughs as these lows are comparatively deeper systems. A northerly component wind also intensifies the rainfall of this system. Easterly troughs and lows also interact with the mid-latitude features forming tropical-temperate features such as Tropical Temperate Troughs (TTTs). These systems can cause widespread rainfall over most of South Africa (Hart et al., 2010; Tyson and Preston-Whyte, 2000; Taljaard, 1996).

Beside tropical troughs and lows, tropical cyclones and ridging anticyclones also contribute to the summer rainfall over South Africa. Tropical Cyclones generally affect the east coast of South Africa and can cause torrential rainfall over the coast and bordering inland areas. Ridging anticyclones can also cause appreciable rainfall as they can bring about advection of moist, unstable air over the eastern areas of South Africa. Widespread rainfall due to ridging anticyclones can occur over this region when changing curvature of flow, orographic uplift and upper level divergence are combined.

1.2.2.2 Winter rainfall synoptic systems over South Africa

During winter the subtropical anticyclones move about six degrees further north which sees the mid-latitude westerlies extend further north too. Also, during winter the extension of these westerlies causes a northward shift of the tropical easterlies which results in the

tropical systems having very little influence over South Africa during this time (Tyson & Preston-Whyte, 2000).

In winter cold fronts, associated with the mid-latitude westerlies, produce areas of substantial convection to the rear of the trough. Frontal systems mainly affect the southern and eastern coastal belts but on some occasions can cause rainfall further inland of South Africa (Taljaard, 1996). Cut-off lows form when middle to upper troposphere westerly troughs deepen into closed circulations that extend downwards to the suface. Cut-off lows can affect many areas of South Africa (Taljaard, 1996) and are mostly experienced during March/April and September/October. They account for most of the rainfall seen during winter in the summer rainfall regions (Tyson & Preston-Whyte, 2000; Taljaard, 1996). These features can result in flash flooding especially below the south easterly side of the low. Surface highs can form below a cut-off low and can result in the intensification of rainfall experienced.

From the above one can see that the rainfall over South Aftica differs from region to region and even the atmospheric circulations causing rainfall is different for certain areas. Since this is the case this study will focus on two regions of South Africa which are highlighted in Figure (1.1). The first is the Western Cape Province of South Africa (WC) and the second is the east coast region of South Africa (EC), which contains parts of the KwaZulu-Natal province, Eastern Cape Province and Lesotho. These two regions were chosen due to the fact that firstly they both receive appreciable rainfall compared to the surrounding regions and secondly because they show very different rainfall regimes - the WC receives winter rainfall whereas the EC is a predominantly summer rainfall region. This will allow us to test whether extreme events in one rainfall regime is more easily simulated than the other. Lastly the WC was chosen because it is one of the most disaster prone provinces in South Africa and the majority of these disasters are floods (Holloway et al., 2010) whilst the EC was chosen as it experiences large amounts of extreme rainfall events and has the highest concentration of informal settlements (Davis, 2011)

1.3 Impacts of Extreme Rainfall over South Africa

Extreme rainfall events have caused devastating destruction in South Africa, especially in rural or urban areas with poor infrastructure and strained water management. Extreme rainfall events can induce floods resulting in the collapse of small dams and reservoirs which puts strain on water resources. Floods can also lead to the displacement of people, especially since more than a hundred thousand people live on floodplains in South Africa (Mason et al., 1999). On February 2011 the South African Weather Service (SAWS) Climate Summary of South Africa commented on the reported impact of floods in South Africa stating that, since December 2010 to February 2011, the estimated cost of destruction on public infrastructure was around R3.6 million. The floods in this period have affected more than 14400 families and more than 13000 houses were damaged. Therefore the social economic impacts of extreme rainfall events are a serious concern in South Africa, especially since flood-related disasters have risen more than five-fold since the 1980s (Shongwe et al., 2009). To illustrate the negative impacts extreme rainfall events can cause, specifically over the EC and WC, some examples of these events reported by SAWS in their monthly climate summaries of South Africa follow:

- On the 25th of June 2007 in Gugulethu, Cape Town, 500 people were left homeless as a result of a storm caused by a cold front and upper air trough that was situated over the Western Cape (SAWS, 2007).

- On the 12th of July 2009 flooding over the Western Cape, caused by a cold front and upper air trough occurring over the south west coast resulted in 9000 shack dwellers being left homeless. About 143 People in Grabouw were forced to leave their homes and 34 families from Jamestown and Stellenbosch were evacuated (SAWS, 2009).

- On the 5th of January 2011 a surface trough situated over South Africa and an anticyclone south east of the country resulted in floods over KwaZulu-Natal which caused five deaths. Later that month on the 17th, 28 municipalities, were declared disaster areas, due to the flooding that had occurred during the month. Over KwaZulu-Natal alone, damage to roads, bridges and other infrastructure amounted

to about R475 million. At least 1472 houses were destroyed and a further 4799 houses were damaged (SAWS, 2011c).

- On the 8th of June 2011 a low pressure system situated over the south eastern interior and a cut-off low in the upper troposphere over the interior lead to heavy rainfall, which resulted in the displacement of over 1400 people in the Eastern Cape and 200 people being evacuated from an informal settlement in KwaZulu-Natal (SAWS, 2011b).

- On the 19th and 20thof November 2011, floods over KwaZulu-Natal killed five people. These floods were caused by a trough situated over central-west South Africa and an anticyclone south east of the country on the 19th; and a trough at the surface extending from further north to a low over the south east coast on the 20th. Later, on the 27th, 700 houses were destroyed, thousands of people were displaced and eight people died due to flooding produced by a surface trough over the interior and an anticyclone south east of the country (SAWS 2011a).

- Heavy precipitation on the weekend of the 6th of July 2012 in Cape Town led to the disaster management team having to help 2500 people from affected areas. Due to the floods, 60 people had to be evacuated and 132 structures were damaged in informal settlements. This event was caused by a cold front and associated upper air trough lying over the south west coast on the first day of the weekend. The next day the cold front moved further east, with a ridging high moving in behind it and the upper air trough lying over the western regions of South Africa. On the 13th of that month, another cold front was situated over the interior with a high ridging behind it, as well as an upper air cut-off low above the western interior. On the 14th the cold front and cut-off low moved eastward while the high continued to ridge in behind it. Over these two days, 2000 residents were displaced in the Eastern Cape due to the heavy rain caused by these systems (SAWS, 2012).

1.4 Predicting extreme rainfall events over South Africa

Developing a reliable tool for predicting extreme rainfall could be very usefull as it would allow infrastructure to be put into place to deal with the events (Goswamiet al., 2006) as well as allow time to warn and help vulnerable communities. A skillful prediction of extreme rainfall events will reduce the risk associated with economic and social decisions (Landman et al., 2005). However, a regional prediction of extreme events with Global Climate Models (GCMs) is difficult because, while GCMs are skillfull in simulating rainfall at global and continental scales, they often overestimate rainfall over southern Africa(Landman & Beraki, 2012). This is due to the coarse resolution of the GCMs ranging from 100-300km, resulting in a crude or distorted representation of atmospheric processes (Landman & Goddard, 2002; Mason & Joubert, 1997), especially convective rainfall systems (Mason &Joubert, 1997). Therefore, there is a need to make use of GCM simulations and obtain regional information, without having to increase the GCMs resolution over the entire globe, as doing so will increase computational power by a large amount.

The above can be obtained by using Regional Climate Models (RCMs) however, despite this there are relatively few studies that have properly investigated the abilities of RCMs to simulate extreme rainfall events over South Africa. In order to properly understand the biases in RCM simulation a study needs to make use of a group of RCMs and needs to focus on specific regions, as RCMs can often do well over some areas and worse over others (Kalognomou et al., 2013). So far studies looking at simulations of extreme rainfall events have only made use of one or two RCMs (e.g. Williams et al., 2011; Joubert et al., 1999). The aim of this study is to evaluate and compare the capabity of CORDEX RCMs in simulating extreme rainfall events over South Africa. The comparison will help indentify which RCMs perform better than the others in replicating the charateristics of the extreme rainfall events. This shall be achieved by analyzing whether there are some inherent biases that can be seen within all the RCMs. This can done by determining whether there are RCMs that do better overall or whether some do better over specific regions and worse over others and by concluding whether some of the RCMs actually improve the lower resolution dataset that is forcing them at the boundaries.

1.5 Aim of the study

The aim of this study is to evaluate the ability of the CORDEX RCMs in simulating extreme rainfall events over the EC and WC. In doing so this study will help to further the understanding of the limitations of using RCMs to simulate extreme rainfall over South Africa and to see whether certain models do better over different regions of the country. Since CORDEX data shall be used for future climate projections this study will also add to the body of work in understanding the limitations of using these regional climate models in future climate projections of extreme rainfall events over South Africa (Kalognomou et al., 2013). To achieve this aim the following objectives are addressed:

- Identify the threshold values of the 95th percentile of rainfall for the years 1998-2008 at each grid point over South Africa for the observed, reanalysis and model data. These values shall be compared to get an idea of where the models overestimate or underestimate these values.
- Compare the frequency distribution of rainfall intensity over the EC and WC regions to understand how well the models simulate the distribution of rainfall over these regions
- Identify widespread extreme rainfall events (WEREs) over each of these regions and find the monthly and annual frequency of these events for each area.
- Use Self Organizing Maps (SOMs) to identify the different precipitation patterns associated with the WEREs.
- Obtain the frequency for each of the associated SOMs nodes to understand whether certain models simulate more WEREs associated with certain rainfall patterns compared to others
- Use reanalysis data to get an understanding of the circulation behind the different rainfall patterns of the SOMs

Chapter 2: Literature Review

This chapter provides a comprehensive review of past studies on extreme rainfall events over southern Africa. In the review, the chapter focuses on various definitions used in indentifying extreme rainfall events, atmospheric features and conditions that result in extreme rainfall, and different approaches to simulating extreme rainfall events.

2.1 Definition used to identify extreme rainfall events

Past studies on extreme rainfall events have used a number of different approaches to define these events (Barnston & Mason, 2011). The events have been defined using their characteristics such as frequency, amplitude and persistence (Klein Tank & Zwiers, 2009). Sometimes extreme events are even identified by their destructive impact on society (Barnston & Mason, 2011). A survey of recent literature on extreme precipitation events suggests three predominant ways to define and therefore identify extreme rainfall events.

The first method identifies an extreme rainfall event by defining a threshold value appropriate to the area of study. Any event during which rainfall exceeds this value is defined as an extreme event. Different threshold values are used for different parts of the world (Dyson, 2009). For example, Dyson (2009) used three different threshold values to define extreme rainfall over the Gauteng province. Significant rainfall had a threshold of 10mm day^{-1}, heavy rainfall had a threshold of 15mm day^{-1} and very heavy rainfall had a threshold of 25mm day^{-1}. It is also common to define threshold values for a specific area size as well as for a specific time span (Dyson, 2009). For example, Engelbrecht et al. (2013) used 20mm to define an extreme daily rainfall event within a 0.5° by 0.5° grid over South Africa. To see how different threshold values can be, one only needs to look at the threshold values defined by Groisman et al. (2001) compared to those mentioned for the Gauteng province by Dyson (2009). Groisman et al. (2001) defines a heavy rain event over the United States as 100 mm per day in a 1° by 1° grid and a very heavy rain event as 150 mm per day in a 1° by 1° grid. Therefore these threshold values are specific to an area as different regions receive different amounts of rainfall. As mentioned in Chapter one, South Africa's rainfall is spatially varied and if one was to use a specific threshold value across South Africa it would be difficult to compare how well the model simulates extreme rainfall events

compared to observed events because using threshold values are less suitable for spatial comparison (Klein Tank & Zwiers, 2009).

The second way of defining extreme rainfall events is by using return periods. Mélice and Reason (2007) used return periods to estimate how often destructive precipitation events occur in George by using a 65 year data series as well as an extreme value model. Mason and Joubert (1997), in a study aimed at analysing the change in extreme rainfall over South Africa, calculated the magnitude of events with 5, 10, 15, 25 and 30-year return periods using Generalised Extreme Value distribution for 28 model years as well as observed data for the control period. Sanderson (2010) used the Generalised Pareto distribution to calculate the magnitude of the extreme rainfall events associated with specific return values from a 46-year dataset. From the above one can see that all these studies used long datasets. This is due to the fact that the statistics in these studies enables them to estimate, for example, return value magnitudes for a return period of 100 years from a 25 year data set. However the larger the return periods the larger the uncertainty, this uncertainty decreases the larger the dataset (Sanderson, 2010). Ideally, defining extreme events by their return periods requires a long rainfall time series. Therefore, since this study makes use of simulation data, a long dataset is not really possible and using this method would result in high uncertainties in the return values.

The third method uses percentiles to define extreme rainfall events. In this method, a rainfall event is extreme if it lies within a certain percentile of the distribution. This is done by ranking precipitation values for the time period from largest to smallest and thus the percentiles are calculated directly from the rainfall distribution. Landman et al. (2005) defines an extreme rainfall season as a season whose rainfall anomalies fall within the top 20^{th} percentile of the climate records. Grimm and Tedeschi (2009) define extreme precipitation as a three-day mean above the 90^{th} percentile. Williams et al. (2011, 2010, 2008) defined an extreme event as 1.5% of the mean. They deemed it an appropriate definition of extreme rainfall because it constituted 10% of the highest rainfall days. According to Williams et al. (2011) this percentage is appropriate for a highly variable region, such as South Africa. Using percentile thresholds is useful as it is meaningful for all regions, unlike fixed thresholds (Klein Tank & Zwiers, 2009) and it does not require long data sets like return periods.

Thus the third method seems to be the best method to use for the purpose of this study. This study shall use the 95th percentile as it is the percentile used by Dyson (2009) to define a heavy rainfall event while the 90th percentile is referred to as a significant rainfall event. Warnings of heavy rainfall are issued at the South African Weather Service(SAWS) if rainfall over any area of South Africa has exceeded 50mm day^{-1} —therefore using the 95th percentile threshold value, over the east coast region (EC) and Western Cape (WC), will include these events and some events that may not have as much rainfall but are still considered extreme.

2.2 Conditions causing extreme rainfall events over South Africa

Some of the past studies on extremes rainfall events over southern Africa have used case studies or specific events to investigate the relationships between extreme rainfall events and some atmospheric features over southern African. For example, Hart et al. (2010) used three cases of extreme rainfall events to explore the influence of tropical-extratropical interaction on extreme rainfall events over southern Africa. The authors describe the typical features seen during a Tropical Temperate Trough (TTT) : The presence of an Angolan low and a weak high pressure over the southern Mozambique area causes higher than usual pressure gradients just north of South Africa which results in north easterly flow over this region. This can result in the flow of tropical easterlies from the north of Madasgcar into the sub-continent. A Kalahari thermal low leads to north-easterly flow occurring further south. A ridging South Atlantic Anticyclone (SAA),the northwestward extension of the South Indian Anticyclone (SIA) and a surface low pressue over the Mozambique channel can result in an easterly wave flowing into Mozambique and the east South African regions. The above typical conditions can lead to a TTT starting at the Angolan low and stretching south eastward over the sub-continent. The study found that the Angolan low played a role in bringing in moisture into the region, where the main source of moisture came from the tropical Indian Ocean. Upper level troughs over South Africa played a huge role in triggering the cloud formation, and heavy rainfall occurred due to advection from temperature gradients and positive vorticity as well as convection (especially in the sub-tropics).

Many studies state that these systems are major contributors to South African rainfall, especially in the summer months (Singleton & Reason, 2007; Dyson & Van Heerden, 2002;

Rouault et al., 2002; Todd & Washington, 1999; Van den Heever et al., 1997). Lennard et al. (2013) showed that TTTs over the south Western Cape region accounted for 35% of the 95th percentile rainfall days in autumn and 46% in spring. Summer also showed higher numbers of extreme rainfall days associated with TTTs but in winter only one extreme rainfall event was associated with a TTT. However, the authors also stated that while some TTTs did show extreme rainfall these were extreme cases and not all TTTs produce these high rainfall amounts. Van den Heever et al. (1997), Hart et al. (2010) and Blamey and Reason (2011) agree that although TTTs are large scale systems they contain convective processes that occur on smaller scales thus higher resolution models will be more advantageous when simulating these events.

Crimp and Mason (1999) studied and simulated the extreme rainfall event that occurred over South Africa from the 11th to 16th February 1996 using the Colorado State University Regional Atmospheric Model (RAMS), a mesoscale numerical model. On the 11th of February conditions very similar to those mentioned for TTTs in the preceding paragraph were present with the addition of a departing cold front. Widespread extreme rainfall occurred over the eastern half of southern Africa, with the highest rainfall values seen over the east coast regions. The next day the ridging anticyclone was subsumed into the SIA and therefore precipitation over the east coast region was reduced. This example shows how important onshore flow onto the east coast can be for extreme rainfall over this region. This also highlights the importance of the moisture being brought in due to the ridging high and the topography of the region which again emphasises the importance of higher resolution modelling to resolve SST and topography gradients. The study also found that for the specific events the east and south east Indian Ocean was a more predominant moisture source for extreme rainfall than the equatorial Indian Ocean. This is different to Hart et al.'s (2010) study which suggests that the combination of the cold front and ridging anticyclone, seen in the study by Crimp and Mason (1999), resulted in more moisture being brought into the eastern regions of South Africa from the south-west Indian Ocean. Rouault et al. (2002) states that the main moisture source over the interior of South Africa for heavy rainfall events is from the tropics, whereas the Eastern Cape's main moisture source is from the south-west Indian Ocean. This emphasises the need for regional studies of extreme rainfall events especially when analyzing Regional Climate Models as a model may over or under

simulate moisture sources in a specific area which is more easily identifiable if a regional study is done rather than a study looking at the country as a whole.

Rouault et al. (2002) states that generally studies of specific extreme rainfall events have been predominantly on TTTs, sub-tropical and tropical cyclones and cut-off lows. However the authors looked at a case where a thermal low over South Africa, a westerly trough and SIA interacted to cause heavy rainfall over the Western cape and later the Eastern cape. The study found that the main moisture feed was from the Agulhas Current rather than the north and north east. The study also showed that because the core of the Agulhas Current is only 100km wide, low resolution simulations cannot accurately resolve the current. Once again this study emphasises the need for regional appropriate, high resolution simulations of extreme rainfall events over South Africa.

Singleton and Reason (2006) studied a severe event over the Eastern Cape to understand how sea surface temperature and topography influence or cause extreme rainfall events. They also concluded that the extreme rainfall events would not have occurred without the Agulhas Current due to the warm SSTs of the current which helped to sufficiently destabilise the atmosphere. Singleton and Reason (2006) also emphasised the effect of the steep topography on the position of the extreme rainfall.

Lennard et al. (2013) looked at the associated circulation patterns of extreme rainfall over different rainfall regions. Over the Eastern Cape the authors found that more extreme rainfall occurred over the summer months; December,January and February, followed by the spring months September, October and November. In summer extreme rainfall is mainly caused by surface troughs over the interior of South Africa and high pressure systems off the east coast. In spring Lennard et al. (2013) state that the dominant circulation patterns for extreme rainfall events are ones that show a ridging anticyclone at the surface and a mid-latitude trough in the upper air. The KwaZulu-Natal region shows a similar seasonal distribution with high values of extreme rainfall occurring in summer and spring. Summer extreme rainfall events are associated with surface troughs extrending from the sub-tropics over the interior and more zonal upper air flow while spring shows ridging high pressure systems with weak mid-latitude troughs above.

Over the Western Cape the highest frequency of extreme rainfall events occur in the winter months, June, July and August. These extreme rainfall events are primarily characterised by mid-latitude cyclones to the south of the country and a high pressure over the interior. This may also include cut-off lows however the study used rainfall regimes instead of extreme rainfall regimes which may have resulted in too few cut-off low events and therefore these events being generalized with other events in the SOMs.

Lennard et al. (2013) used 500hPa geopotential height and Mean Sea Level Pressure to train their SOMs and therefore the different types of events found for each area were identified with similar surface and mid-troposphere pressure patterns. In this study a different approach is taken, where events are grouped by different rainfall patterns. In this way one can see whether certain models are more likely to simulate rainfall in certain patterns compared to others. Since rainfall over South Africa is affected by topography, SSTs, synoptic circulation and different moisture sources perhaps this methodology could provide some idea of where the regional climate models' biases lie.

2.3 Simulating extreme rainfall events

Due to the fact that climate change is projected to change the frequency and intensity of extreme rainfall events, studies on projected changes have received increasing interest worldwide (Rajczak & Schär, 2013). Past studies over South Africa have identified positive trends in extreme rainfall events over the country (e.g. Engelbrecht et al., 2013; Sen Roy & Rouault, 2013; Williams et al., 2011; Mason et al., 1999; Mason & Joubert, 1997). Sen Roy and Rouault (2013) found that the positive trends in extreme rainfall events are highest over the south eastern and south western coasts, suggesting that these areas may be most vulnerable in the future. This validates the two chosen areas of study. Mason and Joubert (1997) projected an increase in the occurrence of extreme rainfall events over southern Africa in the future using a nine level Global Climate Model (GCM), CSIRO, coupled to a single mixed layer ocean model. Williams et al. (2011) suggested that changing SSTs may enhance the larger scale systems that induce extreme rainfall events over the country. This was based on results from a simulation that used the HadAm3 GCM and HadRM3P RCM. Engelbrecht et al. (2013) used a stretch grid model to confirm the possibility of the increase

in cut-off lows over South Africa in the future. The above studies all made use of a single GCM or RCM. However, it has been suggested that using a single model is not sufficient for climate change impact assessments due to the fact that the models have their own internal errors and thus using an ensemble of models may better represent the climate and its variability.

Shongwe et al. (2009) used an ensemble of 12 GCMs from the World Climate Project (WCP) Couple Model Intercomparison Project phase 3 (CMIP3). This study found that extreme rainfall events over the south east and north of southern Africa are projected to become more intense. However, Hudson and Jones (2002) noted that GCMs are not able to resolve the rain causing processes sufficiently enough to be able to predict extreme rainfall behaviour with much skill. While global circulation models (GCMs) are very good at simulating global and synoptic scale features, they peform poorly at simulating local scale features, which usually induce extreme rainfall events (Williams et al., 2007; Denis et al., 2002). Owing to their coarse resolutions, GCMs cannot adequately simulate extreme rainfall events, in that, they usually underestimate the intensity of the events (Hudson & Jones, 2002).

Mason and Joubert (1997) used a GCM (CSIRO) coupled to a mixed layer ocean model to simulate extreme rainfall events and found that while the model seemed to produce localised minima on a coastal grid point on the south coast, it was too sensitive to sudden changes in topography and landscape. This is because the GCM's resolution is too coarse to properly resolve local features (Hudson & Jones 2002). Given that Rouault et al. (2002) and Singleton and Reason (2006) emphasied the importance of the Agulhas SSTs and the steep topography of South Africa on extreme rainfall events (as mentioned in section 2.2), there is a need for adequate representation of topography and SSTs. The impacts climate change may have on these events is of serious concern and therefore there is a need for higher resolution projections but first there is a need to assess the inherent uncertainties associated with these high resolution simulations. This present study is focused in that direction. There are two main ways of getting regional information from GCMs and those are statistical and dynamical downscaling.

2.3.1 A statistical approach to extreme rainfall

Statistical modeling of extreme events makes use of Extreme Value Theory (Klein Tank & Zwiers, 2009). This generally involves the extreme percentiles of interest being estimated by an extreme value distribution (Klein Tank & Zwiers, 2009). These distributions include the Generalized Extreme Value (GEV) distribution and the Generalized Pareto (GP) distribution. In a study over Belgrade the GEV and GP distributions were used to calculate return values. The GEV distribution chooses events as extreme if they have no correlation between them whereas the GP distribution seems to allow for more extreme rainfall events (Tošić & Unkašević, 2012). However, the GP distribution is said to ask for more information which the user should choose, for example the user has to choose an appropriate threshold, whereas the GEV distribution uses the data in the data series more efficiently and this may result in more accurate estimates (Klein Tank & Zwiers, 2009). Sanderson (2010) uses GP distribution to calculate return values as wanted to include more extreme values in the analysis (Brown et al., 2008). Gamma distributions are also used in extreme rainfall event studies as distribution of daily precipitation totals can be approximated by the Gamma distribution assuming that daily precipitation is independent of one another (Groisman et al., 2001). The problem with using this distribution is that daily precipitation is not independent as generally if you have rainfall the previous day you are more likely to get rainfall the next day then rainfall after a non-rainfall day (Groisman et al., 2001). According to Murshed et al. (2011) using the Gamma distribution is cumbersome and therefore investigates the usage of a less Cumbersome Beta distribution. In their study it was found that the Beta-κ distribution is less cumbersome than the Gamma distribution and as effective as the GEV distribution. Mason and Joubert (1997) made use of the Beta-κ (used for annual data) and Beta-P (used for seasonal data) to calculate magnitude of events with specific return periods to analyse changes in extreme rainfall events over South Africa.

The problem with using these methods especially using Extreme Value Distributions is that this theory is more appropriate for events that are rare rather than events that occur a few times a year. Also it seems that these studies require longer data sets for higher accuracy which is not always available. Since this study is over South Africa where there is large spatial variability across the region we are interested in the spatial distribution of extreme events. Forecasting extreme events using statistical methods results in many spatial

contradictions (Goswami et al., 2006). Also statistical methods do not take into account topographical effects on extreme rainfall events. Goswami et al. (2006) concludes that extreme rainfall events cannot be forecasted using methods that do not take into acount the geomorphology of the area being studied. Therefore it would seem that using Dynamical methods would produce better results.

2.3.2 A dynamical approach to extreme rainfall events

To overcome the limitation of GCMs, regional climate researchers often use regional models forced with GCM results to simulate extreme rainfall events. Joubert et al. (1999) used DARLAM, an RCM forced by the output of CSIR09, a GCM to simulate the past and future climate of South Africa. The authors claim that this study was the first of such an experiment over southern Africa and the authors found that the performance of the regional model showed an improvement to the results of the GCM. They also concluded that DARLAM was able to simulate the correct circulation patterns associated with above average rainfall. Despite this, there were issues with simulating the extreme rainfall as the RCM overestimated the amount and frequency of rainfall over most of the eastern parts of southern Africa. This was due to incorrect representation of the steep topography over this region. Williams et al. (2010) compared the simulations of extreme rainfall events between the HadAM3 GCM and the HadAM3P RCM and found that that the RCM was able to simulate more accurately the number of extremes but with its finer resolution some spatial accuracy was lost. While these individual RCMs show greater skill in simulating extreme rainfall events over South Africa compared to the GCMs, it is difficult to pass comment on the general skill of RCMs in reproducting these events as very few multi-RCM studies have been conducted on simulating extreme rainfall over South Africa. Kalognomou et al. (2013) state that in order to really understand the biases associated with RCMs one should use co-ordinated RCM simulations. The authors also state that these analyses should be separated into different regional studies as biases are often seen in RCMs over different regions (Kalognomou et al., 2013).

The Co-ordinated Regional Downscaling Experiment (CORDEX) is a new initiative to output multi-RCM simulation over several domains, one of which being Africa. Nikulin et al. (2012) shows that the CORDEX RCMs show satisfactory results in simulating the general

characteristics of rainfall over Africa. However, the authors state that specific RCMs show noteworthy biases over different regions and seasons. A similar result was found by Kalognomou et al. (2013) in their study which analysed CORDEX's ability to simulate precipitation over southern Africa. Kim et al. (2011) states that the RCMs are able to better simulate rainfall over the west of Africa than the east and that wet biases were simulated over South Africa. In their study it was also emphasised, that impact studies need to do RCM evaluations for specific regions, variables and metrics before they are used for projections because biases may vary for each of these. This study supports this idea as it is looking at the simulation of extreme rainfall, by CORDEX RCMs, over South Africa with an emphasis on the WC and EC.

Kalognomou et al. (2013) suggests that the main source of errors in the simulations of southern African rainfall can be attributed to the internal variability and the selected physics used in the models. They also state that the convective schemes used are of major importance when it comes to the errors observed in the rainfall data. This was also emphasised in Jacob et al's (2013) study of precipitation simulated by CORDEX RCMs over the Europe domain. The convective scheme used in the CORDEX RCMs include Kain-Fritsch, Grell and Fritsch, Tiedke, Bougeault and Gregory and Rountree schemes. The Kain-Fritsch scheme seems to be the convection scheme that does the best over southern Africa (Kalognomou, et al. 2013). Bader et al. (2008) emphasise the fact that performance of convection schemes are region and regime dependent with the Kain-Fritsch convection scheme more sensitive to boundary layer forcing whereas the Grell scheme is sensitive to forcing in the troposphere. This may well be the reason for the Kain-Fritsch convection scheme doing well over southern Africa due to the fact that the interior and summer rainfall regions are affected by convective rainfall. Convection schemes are not the only things that can cause errors in RCMs and one main limitation of RCMs is that they are dependent on the boundary conditions supplied by the forcing data (Bader et al., 2008). Therefore errors in the coarser forcing data are past on to the RCM as well and if the RCM corrects these errors it should be for a difinitive physical reason due to the higher resolution of the RCM otherwise what might seem like a correction could just be an error in the RCM that counteracts that of the lower resolution data (Bader et al., 2008). Since this study is using different CORDEX model data we may be able to get an idea of whether the models

identified in the study by Kalognomou et al. (2013) show the same skill for higher rainfall events and whether different models with different convection schemes do better over the east coast regions compared to the Western Cape.

Chapter 3: Methodology

This chapter describes the data and methods used in the study. It starts by providing detailed information on all the datasets used, including their resolution and sources. Then, it provides a comprehensive description of methods used in analyzing the data, including definitions of local and widespread extreme rainfall events, and the self organizing maps used in classifying the widespread extreme events.

3.1 Data

3.1.1 Satellite data

This study used observed satellite-derived rainfall datasets as an alternative to station rainfall data. Williams et al. (2010) states that these kinds of data provide a viable alternative to ground based data. This is especially true over southern Africa, where ground based data is often at a coarse spatial resolution and is not sufficiently distributed in certain regions. This study used data from the Tropical Rainfall Measuring Mission (TRMM). We used the TRMM 3B-42 product which provides rainfall estimates based on certain merged microwave infrared estimates such as the TRMM microwave imager (TMI), visible infrared scanner (VIRS) and TRMM precipitation radar. The details of this process are explained by Huffman et al. (2007). It should be stated that Nikulin et al. (2012) found that during summer, TRMM underestimates precipitation in the north of southern Africa and Kalognomou et al. (2013) shows that TRMM displays different biases during winter over different regions of the eastern part of South Africa. We used TRMM daily rainfall values—averaged from 3 hourly values—and regridded from a 0.25° X 0.25° to a 0.5° X 0.5° grid for the period 1998-2008.

We also used the Global Precipitation Climatology Project (GPCP) satellite-derived dataset, which uses a combination of geosynchronous satellite infrared readings and low earth polar orbit satelittes to estimate rainfall at a 1° X 1° resolution, at a daily time scale (Huffman et al., 2001). Like TRMM, GPCP also tries to incorporate surface precipitation gauge analyses when possible (Huffman et al., 2007). Sylla et al. (2013) looked at differences in rainfall products over Africa and found that GPCP showed rainfall values closer to rain gauge products than the other datasets analysed. Therefore, for this study we shall use GPCP as

our reference dataset and compare it to TRMM, in order to see the extent of the observational error. We used rainfall data from GPCP for the years 1998-2008 regridded to a a 0.5° X 0.5° grid.

3.1.2 Reanalysis data

We used the European Centre for Medium-Range Weather Forecasts (ECMWF) ERA-Interim (ERAINT) reanalysis. The gridded products from this reanalysis include three-hourly surface products and six-hourly upper air products (Dee et al., 2011). According to Dee et al. (2011), one of the advantages of using reanalysis products is that the reanalysis uses a single forecast model, and, therefore the methods used are consistent throughout the dataset. The ERAINT reanalysis is produced with a data assimilation scheme which updates available observation with prior information from the short-range forecast model every 12 hours (Dee et al., 2011). It is the forecast model equations which makes it possible to get unobserved parameters that are physically consistent. One of the main features of ERAINT is that it uses a 4D-variational approach (Zhang et al., 2013), which allows for observations to have a greater effect on the results. Despite this, ERA-Interim simulates positive biases over the tropical west coast of Africa.This is owing to the fact that the Intertropical Convergence Zone (ITCZ) is generally more northward in ERA-Interim as a result of the simulation of the SIA extending further northward, which in turn pushes the ITCZ further north (Zhang et al., 2013). We used ERAINT daily precipitation (averaged from three-hourly values), 500 and 850hPa geopotential height, 850hPa wind vectors, Convective Available Potential Energy (CAPE) and specific humidity (all averaged from six-hourly values) data for the years 1998-2008 at the ERAINT resolution of 2.5° X 2.5°, regridded to a 0.5° X 0.5° grid.

3.1.3 Simulated data

The simulation datasets are from nine of the RCMs that participated in the Coordinated Regional Climate Downscaling Experiment (CORDEX). CORDEX was formed by the World Climate Research Program (WCRP) to evaluate and improve methods of downscaling global climate projections, and to produce multi-model downscaled regional climate information (Giorgi et al., 2009). While CORDEX includes both statistical and dynamical downscaling models, as mentioned above, we shall only be looking at the dynamical downscaling models. CORDEX consists of two phases. The first involves the models downscaling a reference

period with ERAINT used as a “perfect boundary condition” (Kalognomou et al., 2013; Giorgi et al., 2009). In the second phase, the models are forced with the Global Climate Models from the Couple Model Inter-comparison Project phase 5 (CMIP5), over the period 1951-2100 (Kalognomou et al., 2013). These two phases are completed for a number of domains, with Africa being a priority domain. However, we shall just be making use of the first phase data.

All the CORDEX RCMs have a horizontal resolution of 50km. The model domains are the interior boundaries and do not include the lateral relaxation zones. Therefore no spectral nudging towards ERAINT is done within the domain regions. The simulation domain (about 25^{o}W - 60^{o}E and 44^{o}S – 42^{o}N; Nikulin et al., 2012) is much wider than our study domain (Southern Africa; 0^{o} - 50^{o}E, 40^{o} - 0^{o}S). The model Action de Recherche Petite Echelle Grande Echelle (ARPEGE) is a stretched grid model with a 50km resolution over the domain region. A description of the CORDEX RCMs can be found in table 1.

The RCM datasets used in this study are from daily rainfall simulations by nine models (CCLMcom-CCLM4.8, MPI-REMO, UCT-PRECIS, UQAM-CRCM5, CNRM-ARPEGE5.1, ICTP-REGCM3, KNMI-RACMO2.2b, UC-WRF3.1.1 and SHMI-RCA35; table 1) driven by the ERAINT data. All the simulation datasets were obtained from the Climate Systems Analysis Group (CSAG) of the University of Cape Town.

Table 3.1: List of CORDEX RCMs and their attributes (source: Nikulin et al., 2012)

Modeling Center	Institute ID	Model Name	Projection
Centre National de Recherches Meteorolo-Giques	CNRM	ARPEGE	Polar, stretching
Abdus Salam Internation Centre for Theoretical Physics	ICTP	RegCM3	Mercator
CCLM Community	CCLMcom	CCLM	Rotated pole
Koninklijk Nederlands Meteorologisch Intituut	KNMI	RAMCO	Rotated pole
Max Planck Institute	MPI	REMO	Rotated pole
Sveriges Meteorologiska och Hydrologiska Inistitut	SMHI	RCA	Rotated pole
University of Cape Town	UCT	PRECIS	Rotated pole
Universidad de Cantabria	UC	WRF	Mercator
Université du Québec á Motréal	UQAM	CRCM	Rotated pole

3.2 Methods

3.2.1 Grid point extreme rainfall events

In this study an extreme rainfall threshold value at a grid point is defined as the 95th percentile of the daily rainfall distribution at that grid point. Any rainfall amount equal to or greater than this threshold is considered an extreme rainfall event. We analyzed the spatial distribution of threshold values over South Africa for the observed, reanalysis and simulated datasets. This gave us an idea of the intensity of extreme rainfall events simulated by the RCMs and how this compared to observations. ERAINT was used to see whether downscaling the dataset with the RCMs improved these values. This method also allowed a spatial comparison to see where, over South Africa, the highest and lowest discrepancies lie. Over our two regions of interest we calculated the frequency distribution of rainfall for the observation, ERAINT and RCM datasets. We also calculated the cumulative frequency distribution of rainfall, which allowed us to see, over each region, how the percentile threshold values for each dataset varied from each other.

3.2.2 Widespread extreme rainfall events

In the study, a synoptic or widespread extreme rainfall event (WERE), in either of the two focus domains (EC or WC), is regarded as the simultaneous occurrence of an extreme rainfall event over at least 50% of that regions grid points (Figure 1.1) in a day. The day on which it occurs is regarded as a widespread extreme rainfall day. For each dataset, we obtained the widespread extreme rainfall event days. We compared the overall number and the monthly and annual frequency of widespread extreme rainfall events between observations, reanalysis and the RCMs, in order to get an idea of whether the RCMs are able to simulate widespread extreme rainfall events accurately, and whether they can simulate the seasonal cycle of these events as well as the years during which more events occurred.

The WEREs from the observed, Reanalysis and RCM datasets were extracted and Self Organizing Maps (SOMs) were used to classify the WEREs over each area according to their spatial rainfall pattern. The method of the Self Organizing Map will be explained in the following subsection. The number of days that each node is represented in each dataset is analyzed to understand whether certain RCMs are more likely to simulate certain rainfall patterns. ERAINT variables: Convective Available Potential Energy (CAPE), 500 and 850hPa geopotential height, 850hPa wind vectors and specific humidity, are used to get an idea of the average dynamics associated with each of the SOM nodes.

3.2.3 Self organizing maps

SOMs can be classified as a type of artificial neural network. They can be used to recognize and organize spatial patterns in a dataset (Kohonen, 1990), owing to the fact that a SOM both clusters and reduces the dimension of the input data (Skupin & Agarwal, 2008). This is done by taking input vectors and organizing them into characteristic patterns or nodes. When a SOM is produced using atmospheric data it can be directly interpreted as characterizing different weather patterns (Lennard et al., 2013). Therefore using SOMs is appropriate especially since we want to characterize the rainfall patterns associated with WEREs and see whether the models are able or not able to simulate different patterns.

The SOM maps high resolution data onto a lower dimensional array of nodes. However, before this can be done, each node has to be initialized—either with random values or with

some linear estimate of what the values of the nodes should be (Skupin & Agarwal, 2008; Kohonen, 1990). For example, for our study the first two principal components of our input data were used to initialize the SOM's nodes. The number of nodes in a SOM and the topology of the map are generally predefined. The main types of topology for a SOM are the square, rectangular and hexagonal topologies. The user also determines the amount of training time the SOM receives by choosing the number of training cycles (Skupin & Agarwal, 2008).

The SOM is then iteratively trained which entails the individual input vectors being entered and the node which best matches the vector (in this case the node which has the smallest Euclidean distance between itself and the input vector) is updated by the input vector. Not only is that single node updated, but nodes surrounding that node are updated too (Lennard et al., 2013; Skupin & Agarwal, 2008; Kohonen, 1990). The nodes are updated according to a neighborhood function which results in weighted updates of these nodes. The neighborhood function is dependent on the distance between the node that best matches the vector and the node itself, the time step reached in the iteration, the learning rate as well as the neighborhood radius (Skupin & Agarwal, 2008). The neighborhood radius determines the extent to which a single node can affect other nodes in the SOM. In general, the neighborhood radius should start off high, to induce a rough order, before it slowly decreases to refine the organizational map (Kohonen, 1990). The learning rate of the SOM indicates how quickly the nodes update themselves to the input data. This rate also gradually decreases during the iteration process, as the SOM map settles into a stable formation. The training of the SOM stops when the number of cycles has been completed.

This study makes use of the SOMs technique to classify the underlying rainfall patterns as SOMs has advantages over other clustering analysis (i.e. cluster analysis and EOF) in that it is does not depend on the data conforming to a specific distribution or underlying model (Hewitson & Crane, 2002). In addition, unlike EOF methods SOMs does not assume linearity of the data and also allows for patterns to be extracted that are not necessarily orthogonal to each other. This may lead to more realistic patterns than in EOF techniques (Liu et al., 2006) and also results in patterns with varying similarities to each other being presented in the SOMs map (Yoshihiko et al., 2009). Another advantage is that SOMs outputs its results

in the same format as the input data, making the interpretation easier than that of EOFs outputs, which are anomalies of the input data (Liu et al., 2006).

In this study we produced a SOM for each region by inputting the rainfall data for all the WEREs experienced over that region for all the observed, reanalysis and RCM data. The topography used for the SOMs was rectangular, we chose the number of nodes to be 12 (3X4). Although a smaller number of nodes results in higher generalization of the patterns displayed in the SOM (Lennard et al., 2013), we chose 12, because a higher number of nodes did not represent all of the datasets well. This is owing to the fact that the number of WEREs in each dataset was not large (The highest number of WEREs occurring in one of the datasets was 34).

Chapter 4: Spatial distribution of extreme rainfall over South Africa

This chapter presents and describes the results of our analysis on characterizing the threshold of extreme rainfall events over southern Africa. In the chapters the observed results are compared to the simulated results. The discrepancies between the two observation datasets are discussed and the abilities of the CORDEX models in simulating the threshold patterns are evaluated.

The threshold values of extreme rainfall over South Africa in Figure (4.1) show that, in general, the two observed datasets (TRMM and GPCP) produce similar threshold patterns. The correlation between the threshold values of TRMM and GPCP is very high (r=0.9). However, TRMM generally shows higher threshold values, except off the west coast, which matches the dry bias in TRMM discussed by Kalognomou et al. (2013). Both datasets show a local maximum threshold (about 37 mm day^{-1} in GPCP and 42 mm day^{-1} in TRMM) extending from Mozambique to Madagascar. Since this area is prone to tropical cyclones, the local maximum threshold may be associated with tropical cyclone activities. The discrepancies between the two observed datasets, seen in Figure (4.2), are especially high off the east and south coast of South Africa where a tongue of maximum threshold (> 32 mm day^{-1}) in TRMM extends from Mozambique (around 20^{o}S) southward over the Indian Ocean (down to 40^{o}S). This feature, which may be attributed to the influence of the Agulhas Current and its associated warm sea surface temperatures (SSTs) (Singleton & Reason, 2006; Rouault et al., 2002), is absent in the GPCP results. Hence, the discrepancy between the threshold values of GPCP and TRMM over the Agulhas Current core is up to 12 mm day^{-1}. This discrepancy may be due to the difference in the horizontal resolution of the two datasets. Since TRMM has a higher resolution than GPCP, it may resolve the influence of the Agulhas Current core (which is about 100 km) on the rainfall intensity better. However, the difference between the threshold values of GPCP and TRMM over the Western Cape (WC) is less than 4 mm day^{-1}. Over the east coast region (EC) differences of 4mm day^{-1} are mostly seen, except further north along the coast where biases of 8mm day^{-1} occur.

The reanalysis dataset, ERA-Interim (ERAINT), gives a comparable threshold pattern to that of TRMM, in that, apart from showing the west-east threshold gradient and putting the maximum threshold values over Mozambique and Madagascar, it reproduces the tongue of maximum threshold values over the Agulhas Current area. The correlation between the threshold patterns of ERAINT and GPCP is high (r≈0.8). However, ERAINT simulates lower threshold values than both GPCP and TRMM. The negative bias in the threshold of ERAINT (with reference to GPCP, figure 4.2) is up to -20 mm day^{-1} over Mozambique but it is about -4 to -8 mm day^{-1} over WC and -4mm day^{-1} over EC. The ERAINT biases may be attributed to the low resolution and shortcomings in convective parameterization of the GCM used for ERAINT. According to Zhang et al. (2013) the dry bias over Mozambique is due to the fact that ERAINT simulates a strong South Indian Anticyclone (SIA) extending too far north and pushing the Inter-Tropical Convergence Zone (ITCZ) further north as well. This occurs due to the prescribed SSTs which have warm biases in the tropics. These warmer values result in more northerly flow and weakens the southward cross-equatorial wind in summer which, in turn, results in the more northerly position of the SIA (Zhang et al., 2013).

Most of the Regional Climate Models (RCMs) simulate dry biases over Mozambique which suggests that the error is due to an error simulated by ERAINT. In most of the RCMs we can see a dry bias over the interior and north western regions. Kalognomou et al. (2013) state that this bias may be as a result of the fact that, in some of the RCMs, the Angolan low is intensified. This leads to less moisture being advected into the Angolan region. However, a strong Angolan low can also help to intensify north easterly winds which help to bring moist air into the interior (Hart et al., 2010) so whether this intensification is responsible for the dry interior is unclear. The interior of South Africa's rainfall is mainly convective so perhaps the convective schemes used in the models account (at least in part) for these biases. CCLM and REMO show very similar biases over the interior which is interesting because both RCMs use the same convection scheme. However, RACMO also uses the same scheme and while there are some similarities they are not as distinct as in CCLM and REMO. This suggests that the convection scheme is playing a role in the threshold values simulated over the interior but that other RCM errors are also affecting these values.

The spatial correlation, shown in Figure (4.1), between the simulated threshold patterns of CRCM5, RCA35, REMO and WRF compared to GPCP is 0.9, which is higher than that of

ERAINT (0.8) and the other RCMs. These RCMs simulate the high threshold values along the eastern coast as well as the tongue of maximum threshold values over the Agulhas current better than ERAINT (the maximum bias, ± 6 mm day^{-1}, between the simulated values and GPCP is lower than that of ERAINT). ARPEGE and RACMO simulate the worst patterns because they fail to reproduce the west-east threshold gradient, and they have the highest negative bias (>20 mm day^{-1}). However, the spatial correlation of their threshold pattern with that of GPCP is still high (0.6 for ARPEGE and 0.7 for RACMO). CCLM reproduces the west-east threshold gradient and has a lower threshold bias (within ±12 mm day^{-1}) than that of ARPEGE. It also shows a higher spatial correlation value than ARPEGE (0.8). The major weakness, in the CCLM threshold pattern, is that the high threshold values extend more eastward than observed. The model also simulates a local maximum threshold over the Drakensberg Mountains contrary to the observed pattern. PRECIS and RegCM3 simulate a comparable threshold pattern; both reproduce the east-west threshold gradient and simulate maximum values over the Indian Ocean, but fail to extend the maximum value to Mozambique and Madagascar. The spatial correlation of their simulated threshold is about 0.8 and 0.7, respectively, and their maximum threshold biases are within ±12 mm day^{-1}. Looking at South Africa overall some RCMs do better than others however this kind of approach is dangerous as an RCM can do well overall but perform poorly in a specific region. Hence not only is it important to identify which RCMs do well overall, but one needs to examine the performance of a model regionally. For example, ARPEGE has the lowest correlation between itself and GPCP, yet the biases over the WC are less distinct than that of WRF and REMO, who show higher correlation values. In view of this, the next two paragraphs will focus on the RCM simulations of the threshold values over the EC and WC.

When using CCLM to downscale ERAINT the threshold values, of the EC, are higher than that of GPCP (Figure 4.1 and Figure 4.2), especially over the regions of high topography, seen in Figure (1.1), where the values can be up to 12mm higher. These values are also higher than those seen in TRMM so the bias is larger than the uncertainty between the two observed datasets. Using WRF also increases the threshold values, up to about 8mm, over the east coast region, whilst REMO's overestimations are not as distinct. Using ARPEGE and RACMO to downscale ERAINT does not really improve or worsen the threshold values over this region. Similarly, values for PRECIS and RCA35 show little change to those of ERAINT, except

for the fact that these RCMs show slightly higher threshold values over Lesotho and the northern regions of EC. When REGCM3 and CRCM5 are used, threshold values of 8 and 12mm smaller than GPCP, respectively, are simulated over the west of this region and 4mm higher threshold values are simulated along the coast. Therefore it seems that ARPEGE, RACMO, PRECIS and RCA35 simulate the 95th percentile values over this region better than the other RCMs.

All of the RCMs simulate low threshold values off the north-west coast of southern Africa. These low values are also seen in both of the observed datasets and in ERAINT. Like ERAINT, all of the RCMs simulate drier values over this region as compared to the observed datasets. When ERAINT is downscaled using CRCM5 and REGCM3 these low values are extended too far south along the west coast and into the interior. Both of these datasets show similar biases over the WC when compared to ERAINT. PRECIS, RACMO, WRF and REMO show that these lower threshold values extend too far along the west coast and therefore, underestimate the threshold values over the Western Cape. CCLM, ARPEGE and RCA35 appear to minimize the biases produced in ERAINT over the Western Cape.

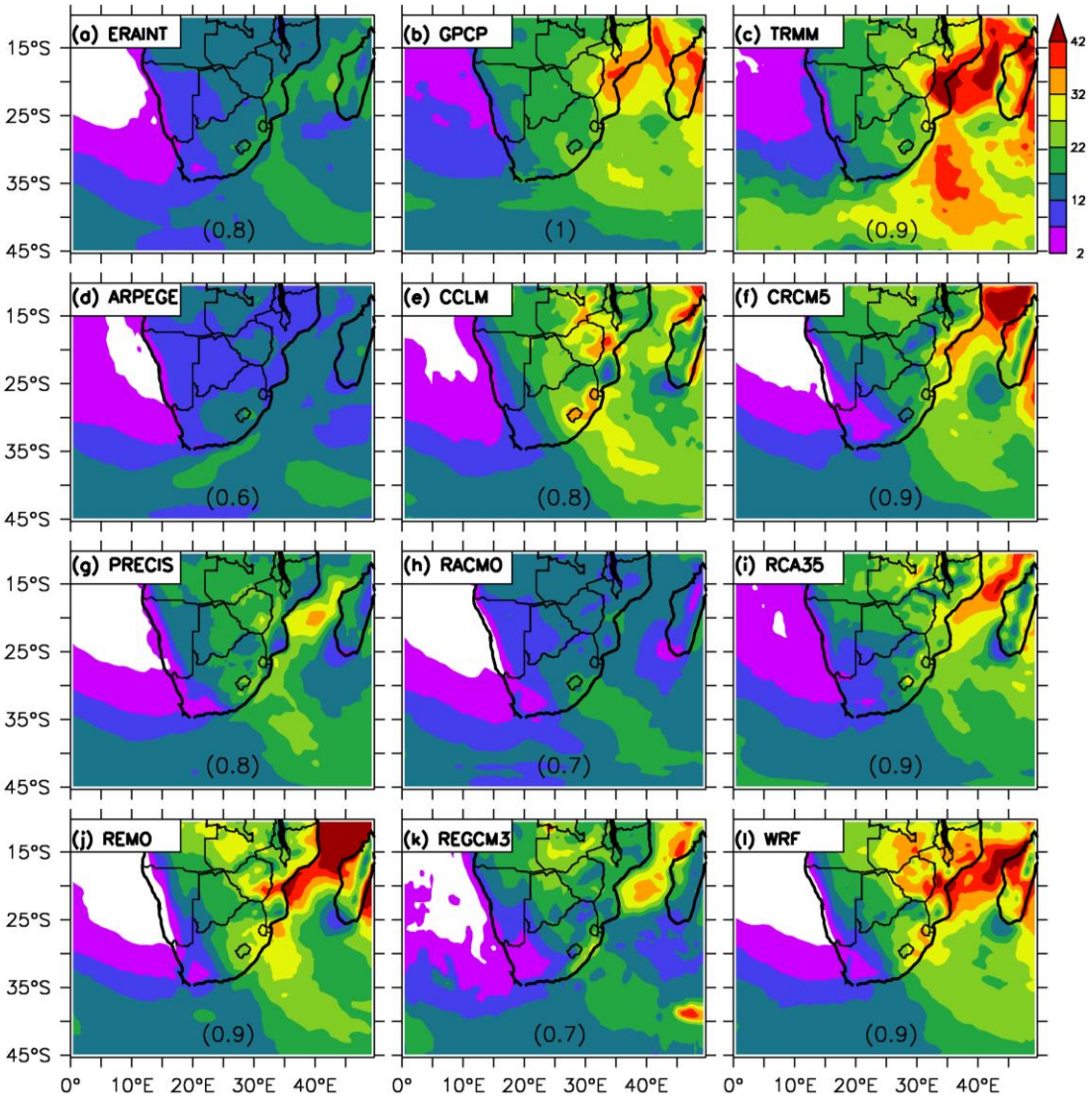

Figure 4.1: The horizontal distribution of extreme rainfall threshold (i.e. 95th percentile) as observed (GPCP and TRMM) and simulated (ERAINT and CORDEX RCMs) over southern Africa for the period 1998-2008. The numbers on each panel show the correlation between the dataset and GPCP. Note that for clarity of presentation, GPCP dataset was correlated with itself

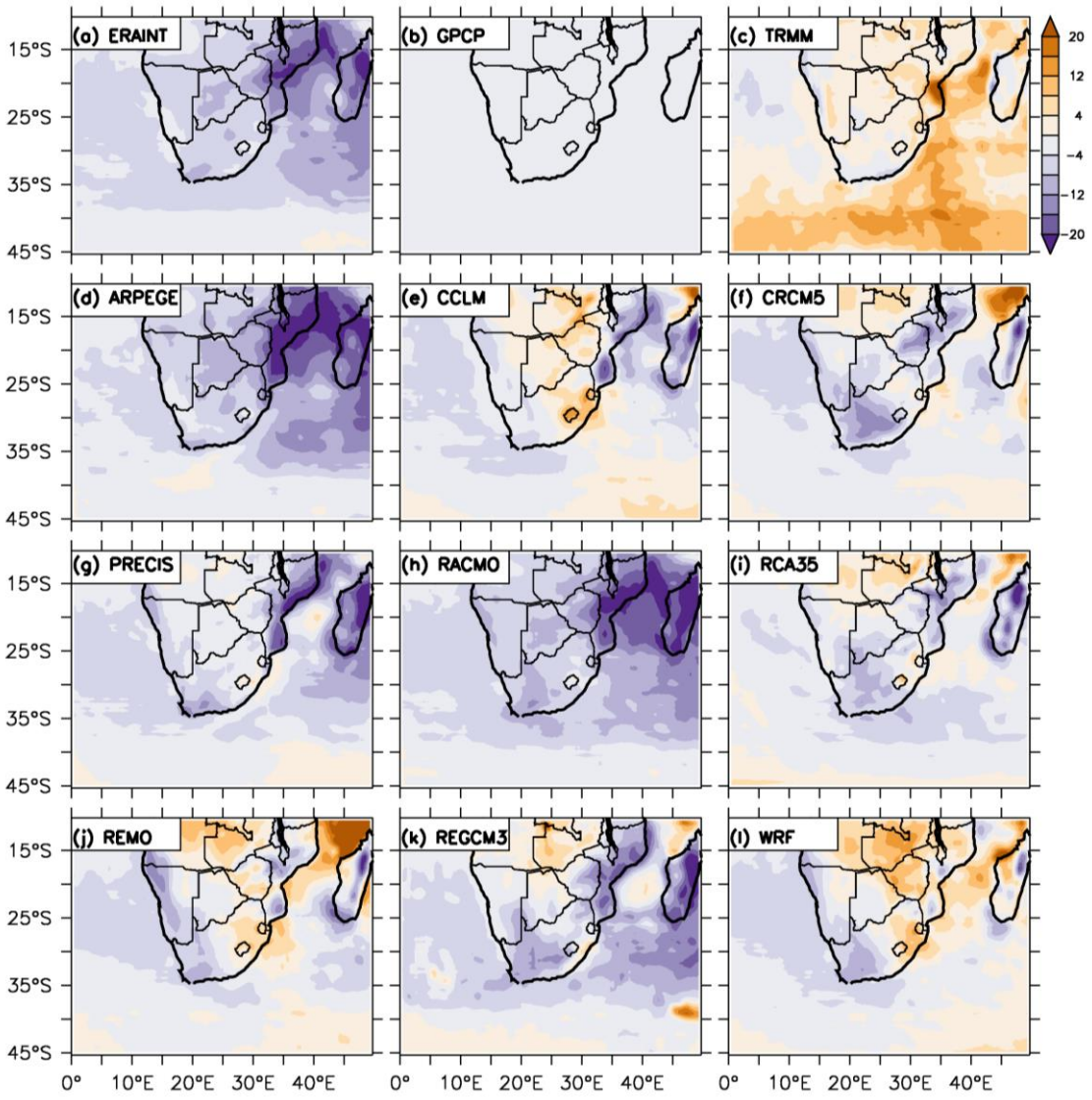

Figure 4.2: The difference between the extreme threshold values of each dataset and that of GPCP (i.e. each dataset minus GPCP) over southern Africa during the period 1998-2008. Note that for clarity of presentation, GPCP data was subtracted from itself.

Chapter 5: Widespread extreme rainfall events over the Western Cape of South Africa

This chapter discusses the characteristics of widespread extreme rainfall events (WEREs) over the Western Cape (WC) as observed and simulated. The characteristics examined include the total number of events, their frequency distribution, their seasonal and interannual variation, and their spatial distribution. In the discussion, the agreements and disagreements between the two observed datasets are indentified and the capabilities of the CORDEX models in reproducing the observed characteristics are presented.

5.1 The frequency distribution of rainfall intensity over the Western Cape

Figure (5.1a) and Figure (5.1b) presents the frequency distribution and cumulative frequency of rainfall intensity over WC as depicted in the observed and simulated datasets. In all the datasets, the frequency of the rainfall decreases rapidly as the rainfall intensity increases, however, the rate of decline varies among the datasets (Figure 5.1a). ERAINT and RegCM3 show the highest rate of decline, whereas TRMM and CCLM show the lowest. This implies that ERAINT and RegCM3 simulate the lowest frequency of intense rainfall events over WC, while TRMM and CCLM produce the highest frequency. This would suggest that downscaling low resolution ERAINT data over WC using CCLM, may enhance the frequency of intense rainfall (and bring it closer to TRMM observation), but using RegCM3 may not. Nevertheless, there are some discrepancies, regarding the distribution of the rainfall intensity: between the two observation datasets (GPCP and TRMM).The frequency decreases faster in GPCP than in TRMM; the greatest discrepancy between them occurs when the rainfall intensity is higher than 60 mm day^{-1}. Despite the discrepancy in the frequency distribution, the cumulative frequency curves for both datasets are very close (Figure 5.1b). For instance, the 95th percentile ($R_{95\%}$) is 20 mm day $^{-1}$ for both datasets. The rainfall cumulative frequency curve for ERAINT ($R_{95\%} \approx$ 12 mm day $^{-1}$) is distinct from that of the observed datasets, and the similar curves for CORDEX RCMs ($R_{95\%}$ is between 8 - 16 mm day^{-1}) cluster around that of ERAINT. RegCM3 simulates the farthest curve ($R_{95\%} \approx$ 8 mm day^{-1}) from the observed while CCLM simulates the closest curve ($R_{95\%} \approx$ 16 mm day^{-1}).

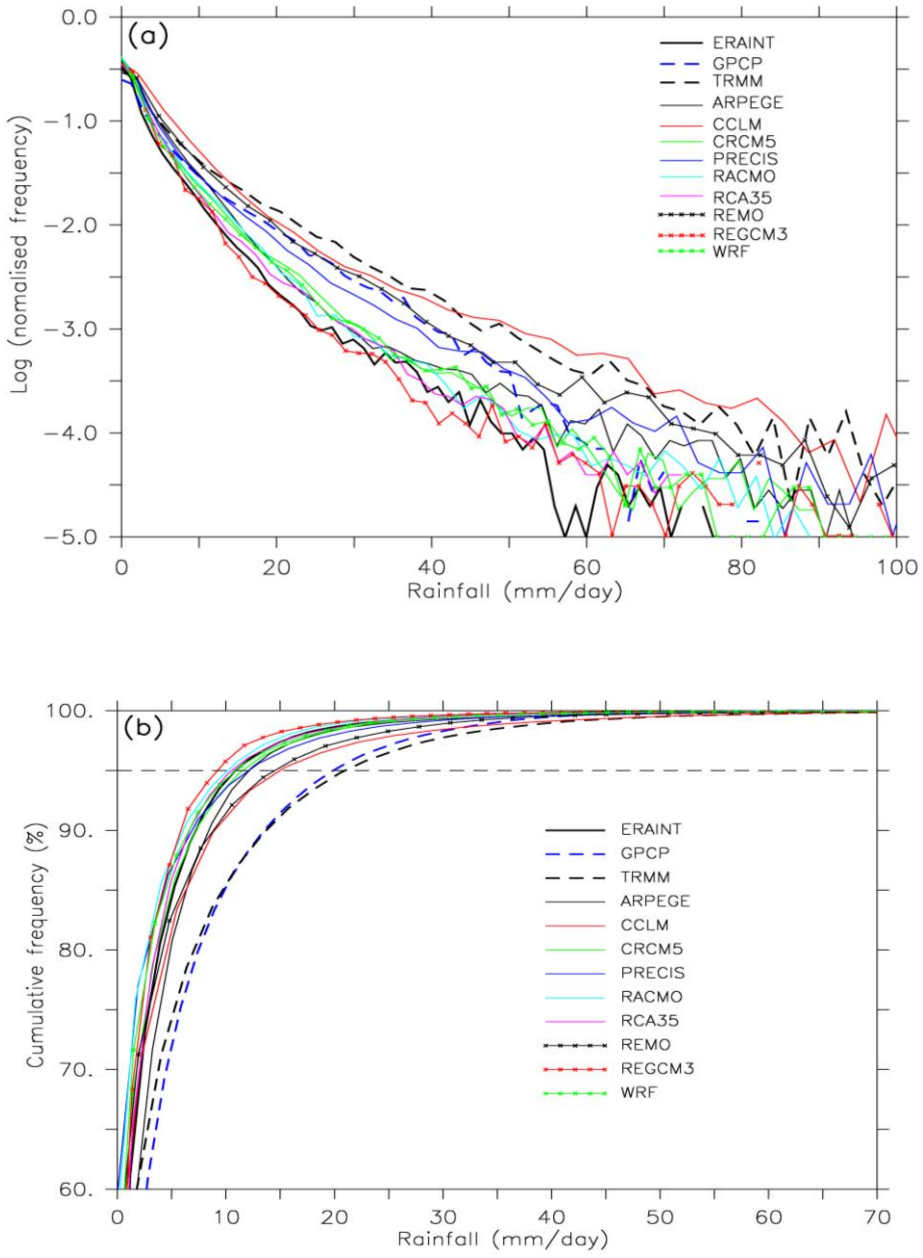

Figure 5.1: The frequency distribution (a) and cumulative frequency distribution (b) of rainfall intensity over the Western Cape (1998 – 2008), for the observed (GPCP and TRMM) and simulated (ERAINT and CORDEX RCMs) datasets. The horizontal dashed line shows the 95th percentile

5.2 The monthly and annual variation of widespread extreme rainfall over the Western Cape

There are some disagreements between the two observations (GPCP and ERAINT) regarding the total number, the monthly distribution, and the inter-annual variation of the widespread extreme rainfall event (WERE) that occurred over WC in 1998-2008 (Figure 5.2). For instance, GPCP reports 24 WEREs but TRMM reports only 7 events (Figure 5.2). In the monthly variation (Figure 5.2), GPCP shows at least one WERE for each month (except for SEPT), but TRMM shows WEREs only occurring in six months (April, June, August and October, November and December). With GPCP, April has the highest number of WEREs (5 events); but with TRMM, August has the highest number of WEREs (2 events). With respect to the inter-annual variation (Figure 5.3), GPCP reports WEREs in every year (except in 1999), as compared to TRMM which only reports WEREs in 5 of the years (1998, 2002, 2004, 2005, and 2008). With GPCP, the highest number of WEREs (5 events) occurred in 2002, 2005 and 2006; but with TRMM, the highest number of WEREs (2 events) occurred in 2002 and 2008. The discrepancy between the two datasets may be attributed to differences in their horizontal resolutions. Despite these differences, there is some consensus between the observed datasets. Firstly, with regards to the monthly variation, GPCP and TRMM both show one WERE in October, November and December. Secondly, in the yearly variation, both show three WEREs in 2008, and agree that 2002 features a maximum number of WEREs.

Figure (5.3) also shows that ERAINT gives a more comparable result (total number, monthly distribution, and annual variation of WERE) to GPCP results than to TRMM results. It reports 27 WERE over WC in 1998-2008, agrees with GPCP that the highest number of WEREs (5 events) occurs in April, and agrees with GPCP (and with TRMM) that 2002 features a maximum number of WERE (4 events). However, contrary to both datasets, it features another maximum value in 1998. Only two RCMs (PRECIS and RACMO) report higher numbers of WERE (34 and 32, respectively) than what ERAINT reports, other RCMs report lower numbers (i.e. ARPEGE: 25; CCLM: 7; CRCM5: 20; PRECIS: 34; RAC35: 13; REMO: 18; RegCM3: 17; WRF: 11 events). This implies that downscaling ERAINT datasets with RCMs may not necessarily increase the number or the spatial coverage of extreme rainfall events over WC. In fact, using CCLM for the downscaling may reduce the number of the simulated

WEREs by more than a factor of 3 (Figure5.3). Nevertheless, given the large disparity between the two observed datasets, it is difficult to ascertain whether the RCM downscaling improves the number of the simulated WEREs or not. More than 65% of the RCMs simulate a total number of WEREs that falls within the range of the observed values. None of the RCMs reproduce the monthly and annual variation of WEREs exactly as in the observed datasets or in ERAINT, but there are a few common features. For instance, in agreement with ERAINT and GPCP, five RCMs (ARPEGE, CCLM, PRECIS, RACMO, and WRF) feature a maximum (or local maximum) number of WEREs (6, 4, 10, 2, and 5 events, respectively) in April. In addition, two RCMs (CRCM5 and REMO) agree with ERAINT on the maximum number of WERE (5 events) in 1998. However, none of the RCMs simulate maximum numbers of WEREs in 2002 as shown by both observation datasets and ERAINT. Hence, on the monthly and annual variation of WERE over WC, there is not much agreement between observation datasets (GPCP and TRMM), nor among CORDEX RCMs simulations.

The results of Figure (5.3) may at first appear contradictory to that of Figure (5.1) because in Figure (5.1) TRMM and CCLM produce higher frequencies of extreme events than those of GPCP and RegCM3, but in Figure (5.3), the reverse is the case. The reason for this is that, while Figure (5.1) reports grid-point based extreme rainfall, Figure (5.3) reports widespread intense rainfall, which is based on the simultaneous occurrence of extreme events in at least 50% of the WC grid points. Hence, while TRMM and CCLM produce a higher number of local (grid-point) extreme events, as compared to those of GPCP and RegCM3, they produce a lower number of widespread extreme events.

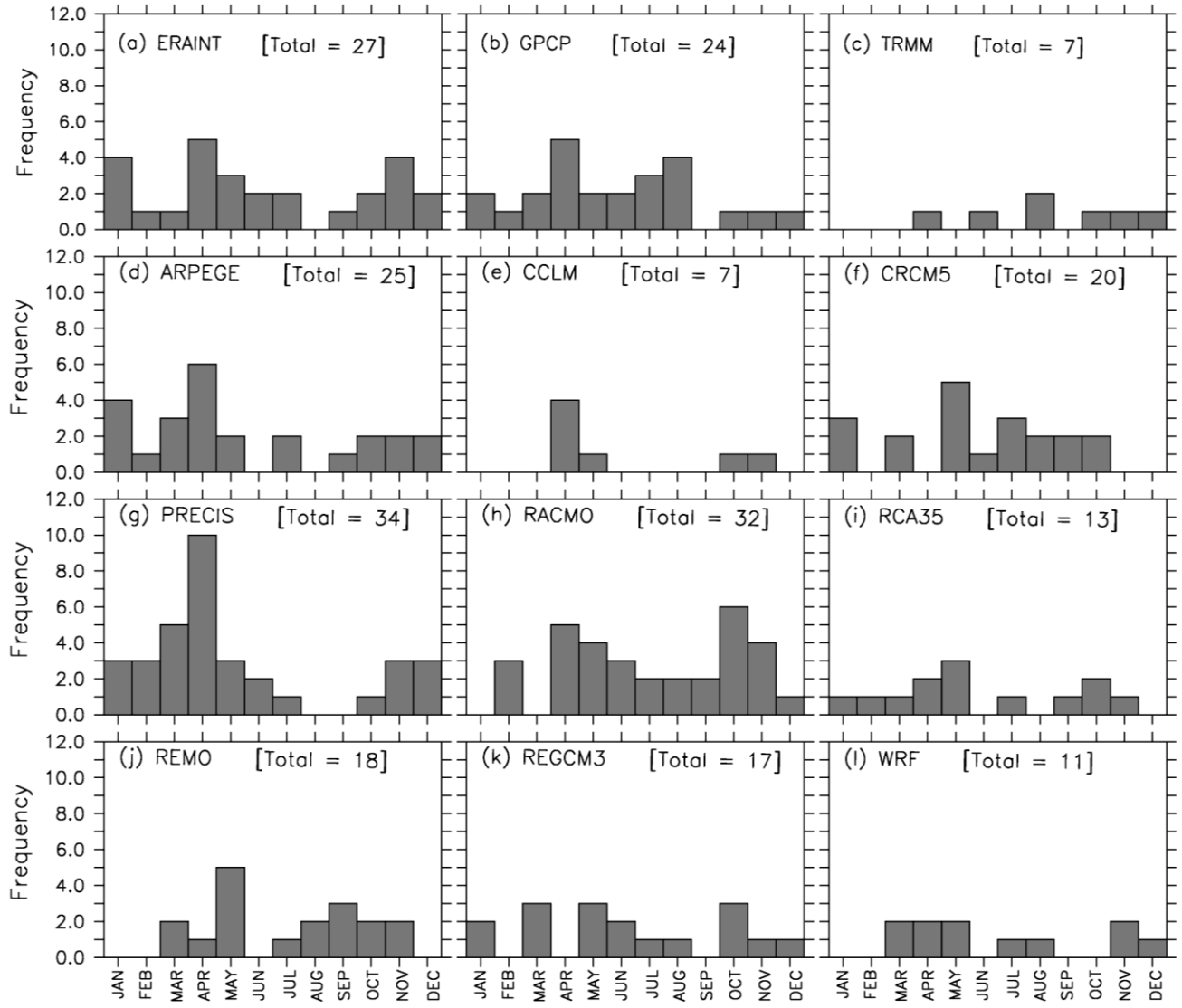

Figure 5.2: The monthly variations of the frequency of widespread extreme rainfall events over Western Cape (1998-2008), as observed (GPCP and TRMM) and simulated (ERAINT and CORDEX RCMs).

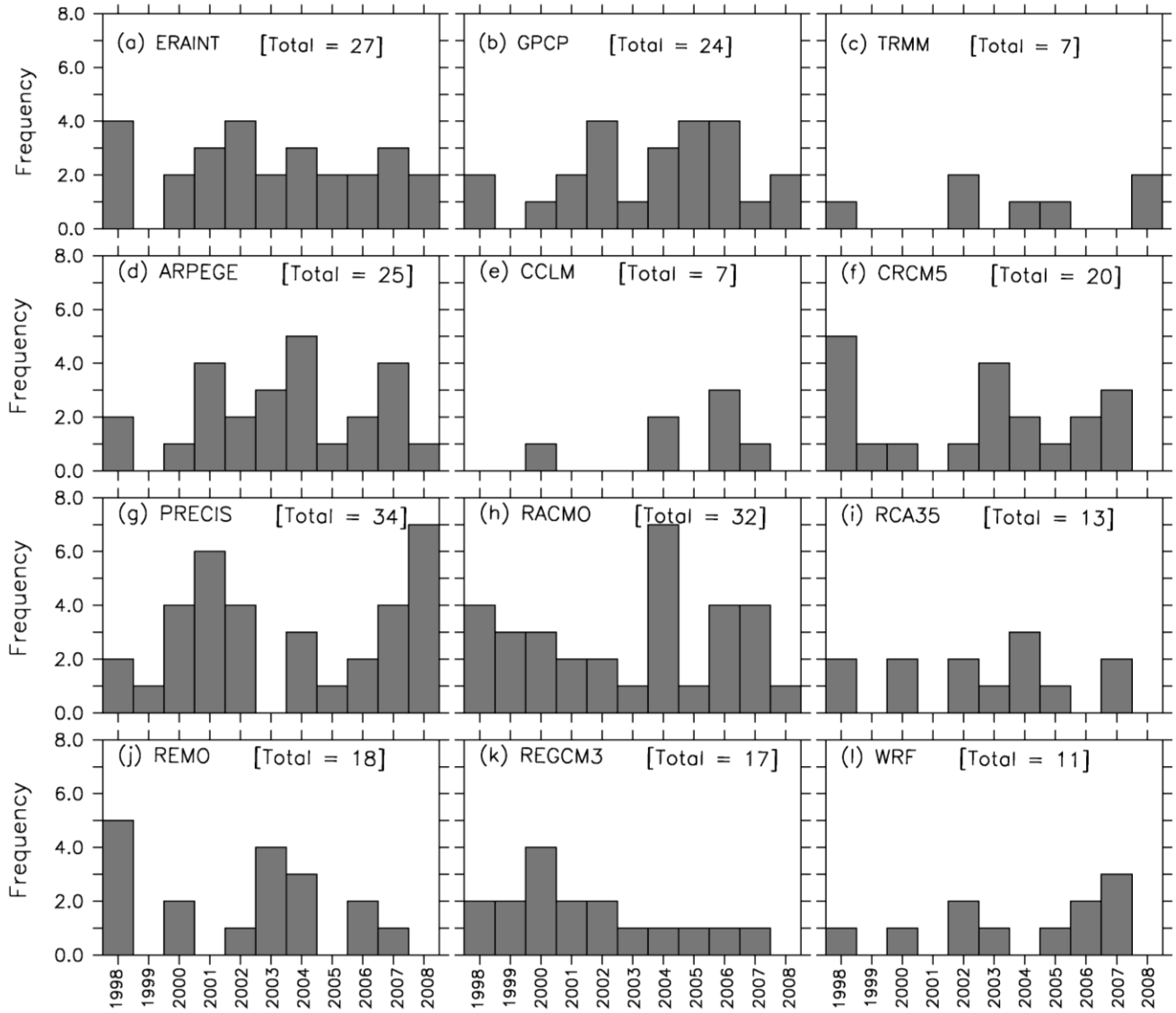

Figure 5.3: The inter-annual variations of widespread extreme rainfall events over Western Cape (1998-2008), as observed (GPCP and TRMM) and simulated (ERAINT and CORDEX RCMs).

5.3 Spatial patterns of widespread extreme rainfall over the Western Cape

Figure (5.4) presents the SOMs' classification of WEREs in the combined datasets (GPCP, TRMM, ERAINT and CORDEX RCMs) into 12 (i.e. 4 x 3) nodes. The classification was based on the spatial patterns of southern African rainfall on the WERE days. A visual inspection of the classification shows that the nodes can be broadly grouped into three categories. The first group (i.e. nodes 1, 2, and 5; hereafter, TRW) features WEREs that are linked with tropical rainfall activities over the continent; in the group, node (1) shows the strongest link between WERE and the tropical rainfall activities. TRW nodes jointly account for 25.5% of the WERE days in the datasets, and node (1) alone accounts for 14%. Figure 5.5 shows that the events in TRW feature in both observation (GPCP and TRMM) and the reanalysis (ERAINT), but they occur more frequently in GPCP (2 and 3 WEREs in nodes 1 and 2, respectively) and ERAINT (7, 2 and 1 WERE in nodes 1, 2 and 5 respectively) than in TRMM (1 WERE in node 5). One RCM (namely, CCLM) fails to simulate WERE in this group. However, among the RCMs that report the TRW events, PRECIS reports the highest frequency (which is higher than observed and that of ERAINT. Further analysis of ERAINT composite data for the WERE days (Figure 5.6-5.8 and Table 5.1) suggest that TRW events are associated with Tropical-Temperate connections and the main source of the moisture is from the Indian Ocean, with additional moisture (evapotranspiration) from Mozambique. ERAINT composite data suggests that these events occur mainly during the summer months, which means that this group is the highest occurring summer group. This is reinforced by a previous study by Lennard et al. (2013), which found that the main summer synoptic conditions causing extreme rainfall events over the South WC are mid-latitude cyclones to the south-west of South Africa connecting to low pressure systems over the interior of the country.

The second group (i.e. nodes 6, 9 and 10; hereafter, ISW) is close to the first group, but features WEREs that have very weak (nodes 6) or no link (nodes 9 and 10) with tropical activities; hence, the WEREs appear isolated; in this regard node (10) features the most isolated WERE. The ISW nodes jointly accounts for 23% of all the WERE days in the combined datasets, but node (10) only accounts for 6.4%. The nodes in this group are well represented by the observation and ERAINT datasets, although, they are more frequent in GPCP (2, 6 and3 WEREs in nodes 6, 9 and 10) and in ERAINT (0, 3 and 5 WERE in nodes 6, 9

and 10) than in TRMM (0, 1 and 3 WERE in nodes 6, 9 and 10). However, TRMM reports its highest number of WERE in this group, especially in node (10). All the RCMs simulate at least one event in ISW nodes; however, only RACMO, PRECIS and REGCM3 simulate frequencies comparable to the observed datasets while the other RCMs, especially WRF and CRCM5, underestimate the frequencies of WERE associated with this group. Figures (5.6) - (5.8) and Table (5.1) suggests that ISW WEREs are associated with a tropical trough or low, bringing in moisture from the Indian Ocean (and from Mozambique) and mid-latitude cyclones centered to the south-west of the WC bringing moisture further south along the west coast. Despite the fact that we see this moisture transport from north to south, we do not see high values of Convective Available Potential Energy (CAPE) all along the tropical-temperate connection as is seen in nodes (1), (2) and (5), which may suggest that these events show weaker connections between the tropics and mid-latitudes and as a result, rain is seen predominantly over the WC. Looking at the dates associated with the ERAINT composite data these nodes are generally associated with spring or autumn months and the synoptic features found for these nodes match those described for the WC during spring and autumn in the study by Lennard, et al. (2013). The fact that these nodes occur during the shoulder seasons also explains why high rainfall over the tropics is not seen in these nodes.

The third group (i.e. nodes 3, 4 and 7; hereafter, MLW) features WEREs that are linked with rainfall activities in the mid-latitude (i.e. over the South Indian Ocean); the link is strongest in node (4). MLW nodes jointly account for about 26% of the WEREs in the combined datasets, out of which node (4) accounts for 9.8%. In this group, GPCP reports two events, TRMM reports one event, while ERAINT reports seven events. Most of the RCMs, except for CCLM, simulate more WEREs associated with this group than the observed data; however, RACMO, CRCM5 and REMO simulate frequencies higher than ERAINT as well. The composite of ERAINT results (Figures 5.6-5.8 and Table 5.1) for MLW indicates that MLW WEREs usually occur in April – July and September – November, and are associated with mid-latitude cyclones that occur across the South coast and extend further north over the east coast which results in moisture being transported from the Atlantic Ocean mostly off the west coast and further south west of South Africa. Reason et al. (2006) emphasise the importance of the South Atlantic Ocean as a moisture source for mid-latitude cyclones and Tyson and Preston-Whyte (2000) emphasise the relationship between the mentioned areas as having a

positive affect on rainfall over South Africa. Lennard et al. (2013) state that extreme rainfall events over the south Western Cape during the shoulder seasons are caused more by summer synoptic conditions which could be a reason why the observed datasets show such few WEREs associated with this, more winter-like, group.

The fourth group (i.e. nodes 8, 11 and 12; hereafter, ACW) is close to MLW in that it shows WEREs that are linked with rainfall activities in the mid-latitude, but in addition, it features strong rainfall activity over the Agulhas Current core, south of the continent. Node (12) shows the most intense rainfall activity over the Agulhas Current core. The three nodes in ACW represent 25% of WEREs in the combined datasets, while node (12) alone accounts for 12%. In this group, GPCP reports six events, TRMM reports one event, while ERAINT reports three events. Most of the RCMs simulate the number of WEREs associated with this group within the observed uncertainty, except for ARPEGE, RACMO, RCA35, PRECIS and REMO which simulate values higher than GPCP. These discrepancies are seen mainly in node (11). The ERAINT composite data shows that the nodes in this group are characterized by strong mid-latitude cyclones (nodes 8 and 11) or cut-off lows (node 12). They also all show south westerly flow over the WC with the Atlantic Ocean to the south west of the region being the major source of moisture. The dates associated with these nodes also show that they occur in either the shoulder months or winter months of the year.

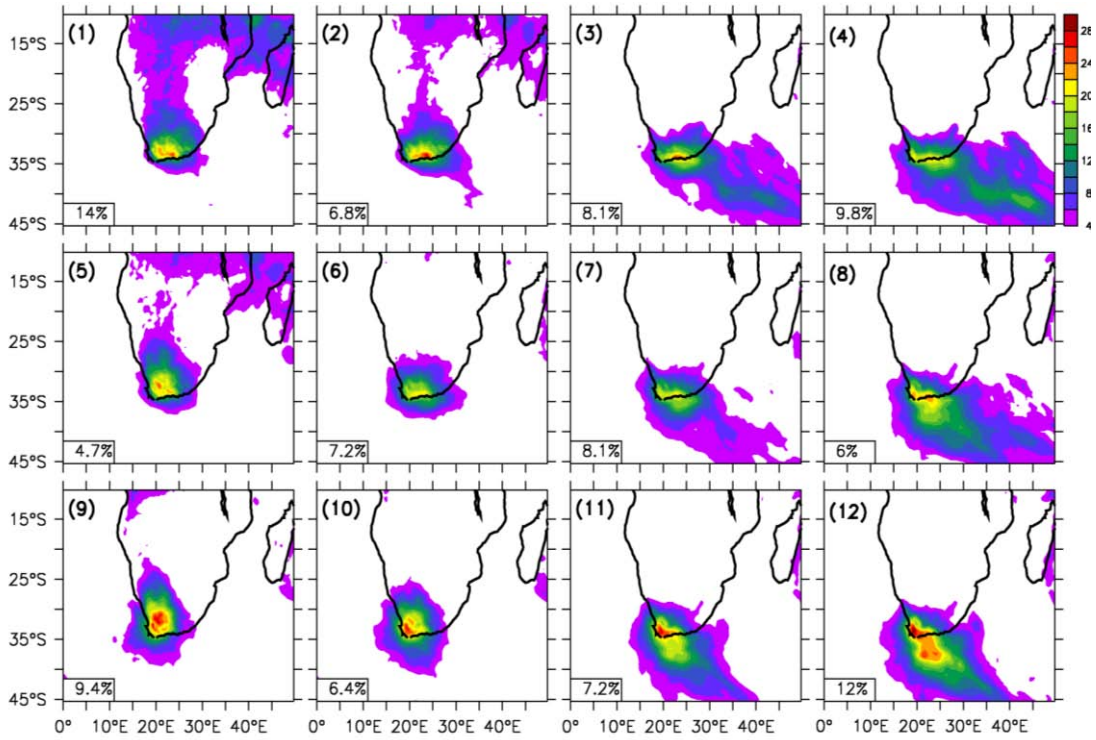

Figure 5.4: The SOMs classification (nodes) of widespread extreme rainfall events in Western Cape (1998-2008), obtained using both observed and simulated datasets.

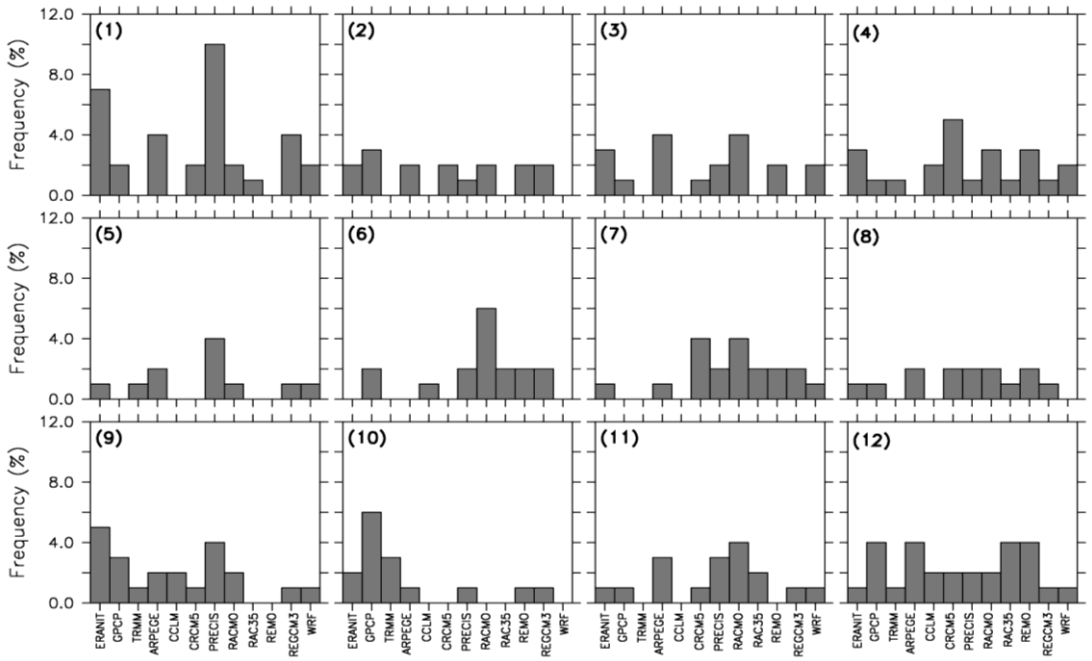

Figure 5.5: The frequency of the SOMs nodes (shown in Fig.5.4) in the observed (GPCP and TRMM) and in simulated (ERAINT and CORDEX RCMs) datasets.

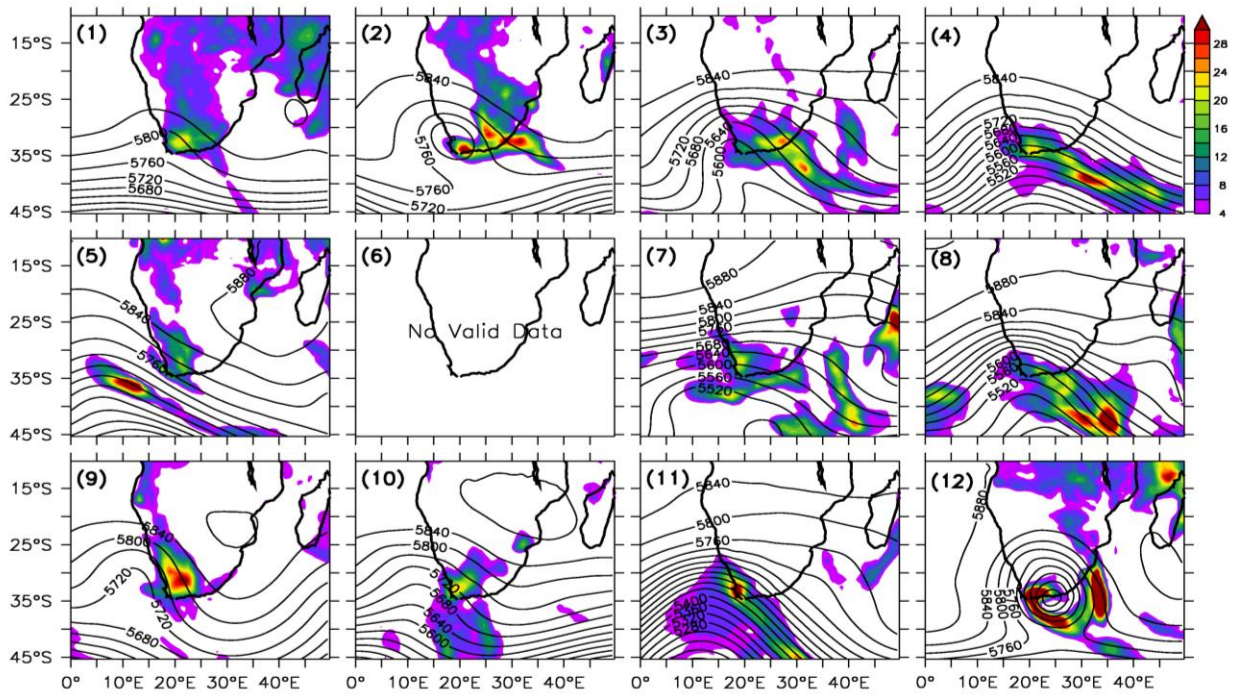

Figure 5.6: The composite of ERAINT rainfall contribution in the SOMs nodes (shown in Fig. 5.4) and the associated 500-mb geopotential heights.

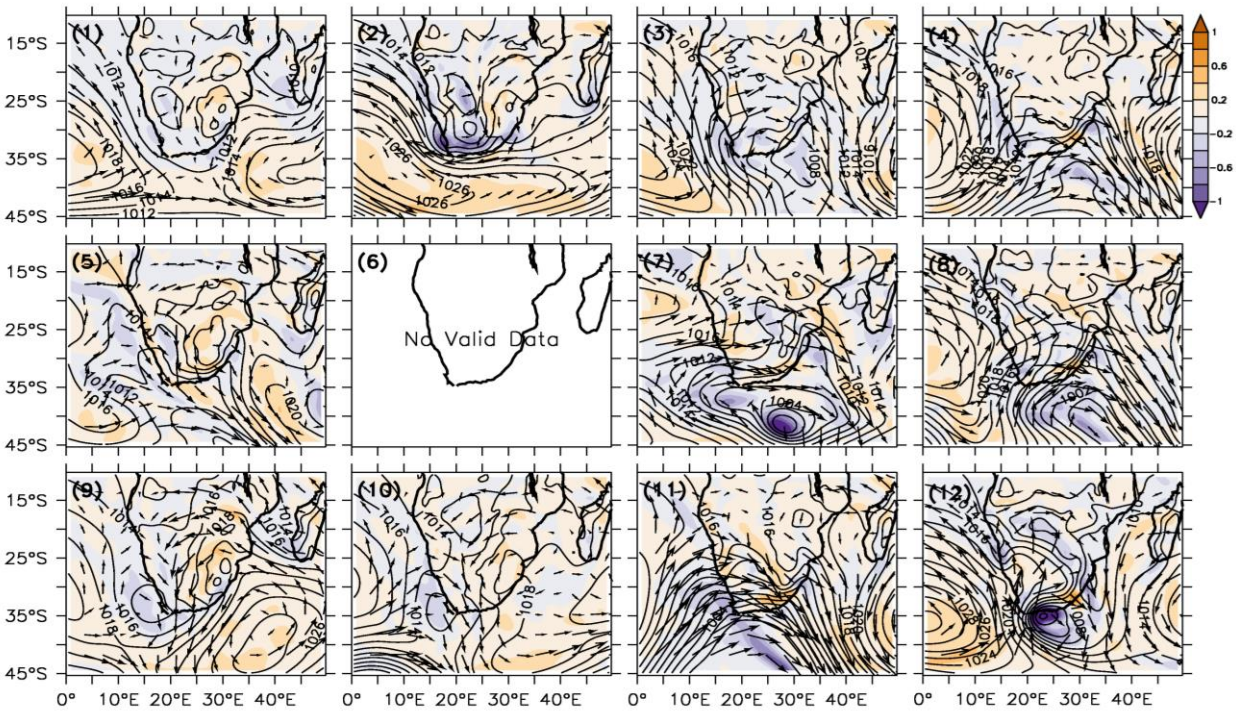

Figure 5.7: Same as Fig 5.6, but for the associated surface pressure (contour) and surface winds (arrows).

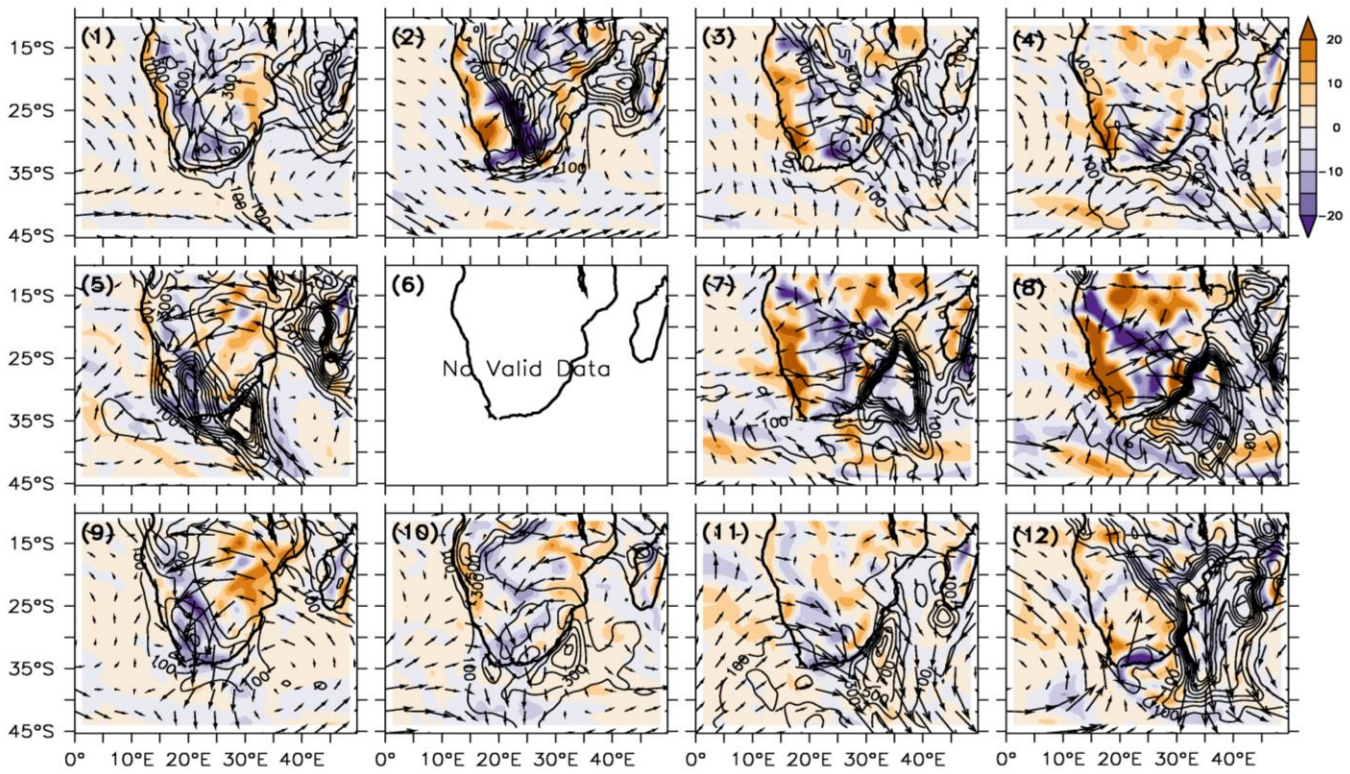

Figure 5.8: Same as Fig. (5.6), but for the associated CAPE (convective available potential energy (J/Kg), moisture fluxes (arrows) and moisture flux convergence (MFC; $\times 10^{-6}\mathrm{Kg}^2\mathrm{m}^2\mathrm{s}^{-2}$).

Table 5.1: Summary of Synoptic conditions seen for each node for Figures 5.6-5.8

Group	Node	Associated Synoptic Features
TRW	1	• At 500mb: weak westerly waves with a trough over WC • At surface: TTT extend from 5°N to South of 45°S, and passes through WC • High CAPE and MFC along the TTT and MFD over Mozambique
	2	• At 500mb: Cut off low within a westerly wave over WC • At surface: SAA and SIA joined and ridging over east, south and south west coast, cut-off low subsumed into a west coast • 850hPa winds show tropical-temperate connection with high vorticity over south coast • High CAPE and MFC values along the west coast trough • Moisture flux shows transport of moisture from the tropics south and from the Indian Ocean above Madagascar and all along the east coast from 15°S to 25°S.
	5	• At 500mb: westerly wave centered to the west of WC • At surface: Ridging anticyclone ridging over most of the eastern regions of

		sub-continent, mid-latitude cyclone further south with a low over the west coast connecting to a tropical trough over the west coast • 850hPa winds shows convergence further north as the winds flow from Atlantic and Indian Ocean and then south along the west coast • High CAPE and MFC values along the west side of South Africa and south coast • Moisture flux shows water coming in from above Madagascar and the south to WC • Some moisture from the Atlantic as well
ISW	9	• At 500mb: westerly trough centered to the west of the west coast of South Africa • At surface: Ridging Anticyclone over east coast region, closed low off the south west coast subsumed within a west coast trough • 850hPa winds show flow from Indian Ocean down along the west coast trough and then cyclonic flow from Atlantic ocean around the closed low • Moisture flux from the Indian Ocean from 15°S to 25°S into the west coast trough, MFD over Mozambique suggests some moisture input due to evapo-transpiration
	10	• At 500mb: westerly trough with center just to the west of WC • At surface: Ridging Anticyclone over most of the eastern side of southern Africa, closed low off the south west coast with the SAA ridging behind it • 850hPa winds show southerly flow over most of the subcontinent due to the ridging anticyclone and onshore flow onto the west coast due to the cyclonic flow associated with the closed low. • High MFC over WC with moisture coming from Indian Ocean due to the ridging high and some moisture from the Atlantic. • MFD over Mozambique suggests some moisture input from this area due to evapotranspiration • CAPE is not particularly high compared to some of the other regions
MLW	3	• At 500mb: westerly trough over WC • At surface: mid-latitude cyclone to the south-east of WC with SAA ridging behind it • 850hPa winds over south WC are meridional Due to the SAA ridging behind the mid-latitude anticyclone • CAPE is not particularly high compared to some of the other regions • Moisture flux show moisture coming from the Atlantic and some from the Ocean south of WC • MFD seen along the west coast
	4	• At 500mb: westerly trough trough across South Africa with axis centered over west coast • At surface: mid-latitude cyclone over east coast with a ridging anticyclone ridging behind it • 850hPa wind shows south westerlies and westerlies over the WC • CAPE is not particularly high compared to some of the other regions • Slight MFC over WC with moisture coming from the Atlantic and some

		from the Ocean south of WC • MFD seen along the west coast
	7	• At 500mb: weak westerly trough over south west coast with a possible cut-off low further south • At surface: mid-latitude cyclone over WC, south coast and east coast with evidence of a cut off low 45°S • Westerly winds across WC at the 850hPa level • MFD along west coast and MFC along the south coast, interior and east coast • Moisture coming from the ocean west of WC
ACW	8	• At 500mb: westerly trough over WC • At surface: mid-latitude cyclone over south-east coast with SAA ridging behind it • Westerly and south-westerly winds over WC at the 850hPa level • High CAPE values over south and east coast. • MFD along west coast and MFC along south coast, interior and east coast • Moisture flux shows moisture coming from Ocean south west of WC
	11	• At 500mb: strong westerly trough centered to the west of WC • At surface: strong mid-latitude cyclone over WCs • 850hPa winds show a mostly westerly flow over WC • CAPE values not as high over the WC compared to the east coast and further south of WC • MFC over WC and MFD to the west and south of WC • Moisture flux shows the Ocean to the south west of WC as the main moisture source
	12	• At 500mb: Cut-off low centered over the south coast • At surface: Cut off low centered a little further east compared to its position in the mid-troposphere, SAA ridging behind cut off low • 850hPa winds show mainly southerly winds over WC • High MFC over south coast and relatively higher values of CAPE over this region too • Moisture coming from Agulhas to the south of the south coast

Chapter 6: Widespread extreme rainfall events over the east coast region of South Africa

This chapter discusses the characteristics of widespread extreme rainfall events (WEREs) over the east coast as observed and simulated. The characteristics examined include the total number of the events, their frequency distribution, their seasonal and interannual variation, and their spatial distribution. In the discussion, the agreements and disagreements between the two observed datasets are indentified and the capabilities of the CORDEX models in reproducing the observed characteristics are presented.

6.1 The frequency distribution of rainfall intensity over the east coast region

Figure (6.1) presents the frequency distribution and cumulative frequency distribution of rainfall intensity, over the east coast region (EC) of South Africa, for the observed and simulated datasets. The figure shows a general decrease in rainfall frequency as the rainfall intensity increases (Figure 6.1a). In general, the curves are similar to those over Western Cape (WC; Figure 5.1a), except for some notable differences (compare Figures 5.1a and 6.1a). For instance, the decrease of the rainfall frequency with the rainfall intensity over EC is slower than that over WC, indicating that EC experiences higher frequency of intense rainfall than what WC experiences. Over EC, after 40 mm day^{-1}, GPCP reports the lowest frequency among all the datasets, in contrast to what happens over WC, where ERAINT reports the lowest frequency after 50mm. Three RCMs (PRECIS, REMO, WRF and CCLM) simulate higher frequencies of $\geq$ 40 mm day^{-1} rainfall than ERAINT, over EC, whereas, over WC all RCMs, except for CCLM, simulate lower frequencies than that of TRMM. However, as deduced over WC, downscaling ERAINT results with RCMs will enhance the frequency of intense rainfall over the EC. Downscaling ERAINT, over EC, using ARPEGE produces the least changes in the frequency curve, while CCLM produces the largest changes.

In addition, the cumulative frequency curves over WC (Figure 5.1b) and EC (Figure 6.1b) also show some notable differences. For instance, while the curves of GPCP and TRMM show a close agreement over WC (Figure 5.1b), they diverge over EC, where all ERAINT and all the RCMs (WRF and REMO) show comparable curves with that of TRMM (below 10 mm day^{-1}) and GPCP is seen as an outlier. Nevertheless, the 95^{th} rainfall values for the two observed

datasets over EC are very close (GPCP: 20 mm day^{-1}; TRMM: 22 mm day^{-1}). Among the RCMs, CCLM gives the highest value (about 27 mm day^{-1}) while ARPEGE gives the lowest value (20 mm day^{-1}). These values are lower than those reported by Lennard et al. (2013), where the EC shows 95^{th} percentile threshold values of about 44mm. This could be due to the fact that they used station data to calculate these values and many of the stations are either at the coast or over the eastern escarpment which may result in higher rainfall amounts.

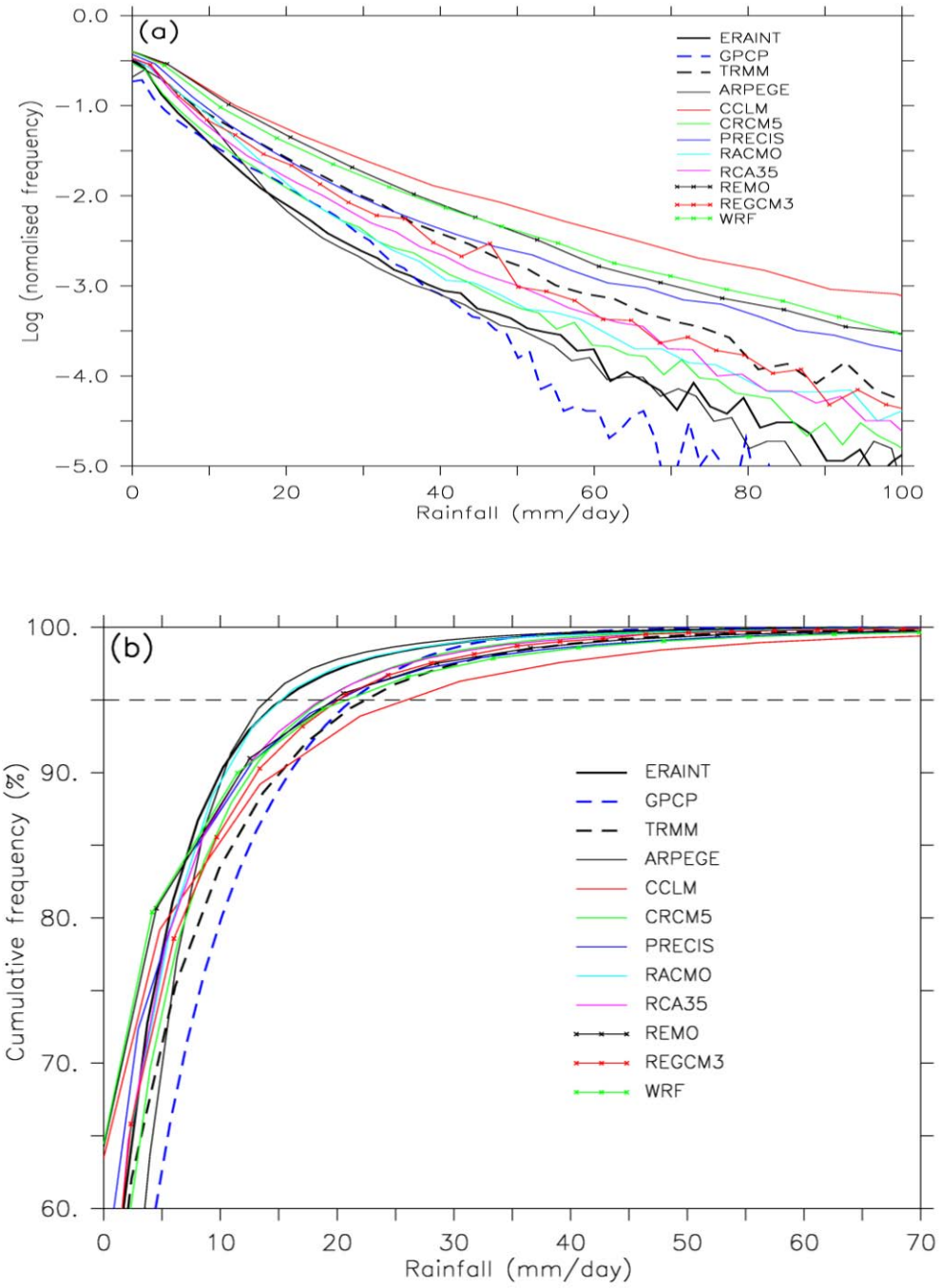

Figure 6.1: The frequency distribution (a) and cumulative frequency distribution (b) of rainfall intensity over the east coast region (1998 – 2008), as observed (GPCP and TRMM) and simulated (ERAINT and CORDEX RCMs). The horizontal thin dash line indicates the 95th percentile.

6.2 The monthly and annual variation of widespread extreme rainfall over the east coast region

Figure (6.2) presents the monthly and inter-annual variability in widespread extreme events (hereafter WEREs) over EC as observed (TRMM and GPCP) and simulated (ERAINT and RCMs). TRMM and GPCP show some differences in the total number,monthly and the inter-annual distribution of WERE that occurred over the east coast region during the period 1998-2008. The most obvious difference is that TRMM reports only three WEREs while GPCP reports seventeen WEREs. This means that even though TRMM shows higher frequencies of intense rainfall (than that of GPCP), as discussed in section 6.1, it reports lower frequencies of widespread intense rainfall over EC, which is consistent with what was found over WC. Hence, while TRMM reports a high number of local gridpoint extremes events over EC, it rarely reports WEREs over EC. The three WEREs of TRMM occur in January, April and November; meanwhile, GPCP reports the peak values of WEREs in March (five events) and November (four events). However, GPCP shows no WEREs in April-July, September and December. ERAINT and all the RCMs vaguely reproduce the monthly distribution of WERE as reported by GPCP (Figure 6.2). ERAINT reports 25 WEREs and puts the peak of the WERE (i.e. four events) in September, December and January. ARPEGE also produces 25 WEREs, but simulates a higher number of WEREs in November (seven events) and December (five events). Among the RCMs, PRECIS produces the highest number of WEREs (27 events) and the peaks of the WEREs are in February (six events) and November (seven events). On the other hand, out of all the RCMs, CCLM produces the least amount of WEREs (only three events in summer; i.e. December - February).

Figure (6.3), which presents the inter-annual variability of the observed and simulated WEREs over EC, shows that both GPCP and TRMM agree that the occurrence of WEREs were higher in 1998, 2000 and 2006. ERAINT and ARPEGE also agree with that, but in addition, they simulate above average values in 2001. The year 1998 was considered a strong La Niña event and this extended into the years 2000 and to some extent 2001. Generally La Niña is said to bring higher rainfall amounts to the east of South Africa (Tyson & Preston-Whyte, 2000) however, whether this also means more extreme rainfall days is still unknown. To an extent, all RCMs (except REMO and CCLM) capture the variabilty in that they simulate above average WEREs in one or two of those years (i.e. 1998, 2000, 2006, 2001), but none of them

perfom better that ERAINT in reproducing the observed (GPCP) inter-annual variability. REMO shows one event in each WERE month, except in December when it shows two events. CCLM on the other hand,simulates two events in 2003 and one in 2000. Hence, among the RCMs, ARPEGE simulates the best inter-annual variablity of WERE over EC, with reference to GPCP observation. However, ARPEGE does not out-perfom ERAINT in simulating the inter-annual variability of the WERE. This implies that downscaling ERAINT results with RCMs may not improve the inter-annual variability of the simulated WEREs over EC.

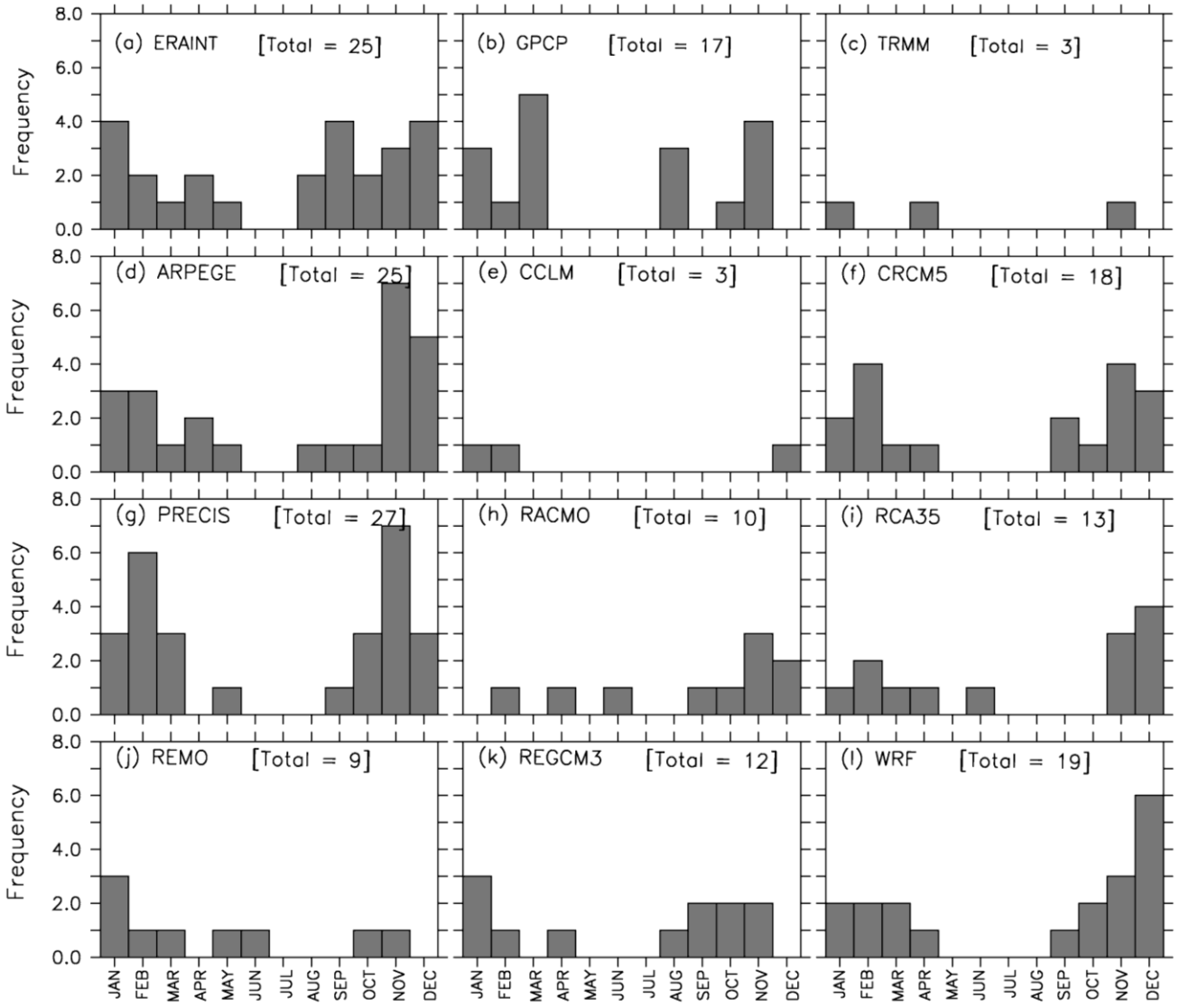

Figure 6.2: The monthly variations of the frequency of widespread extreme rainfall events over the east coast region (1998-2008), as observed (GPCP and TRMM) and simulated (ERAINT and CORDEX RCMs).

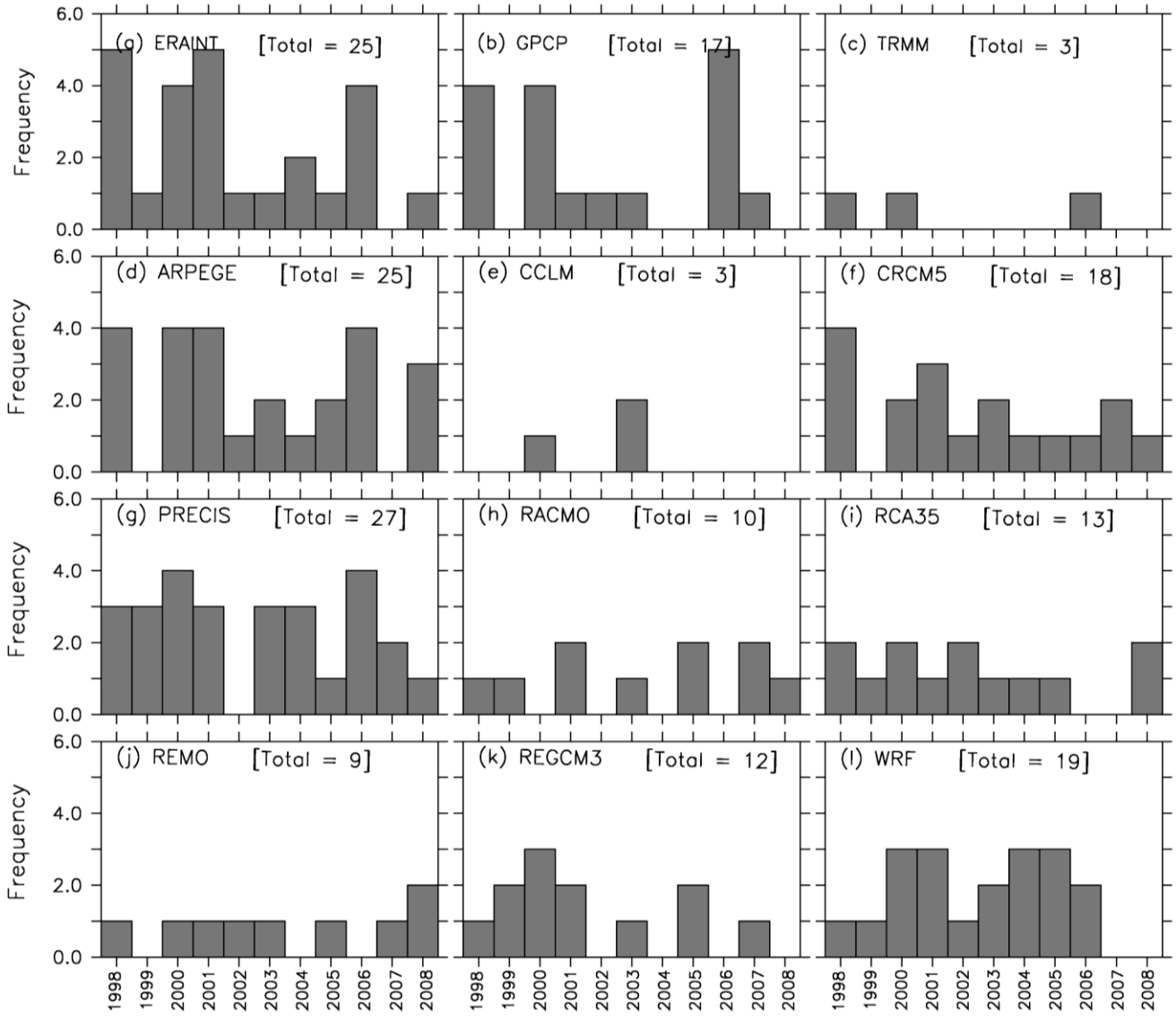

Figure 6.3: The inter-annual variations of widespread extreme rainfall events over the east coast region (1998-2008), as observed (GPCP and TRMM) and simulated (ERAINT and CORDEX RCMs)

6.3 Spatial patterns of widespread extreme rainfall over the east coast region

The SOMs classification of WERE over EC for the combined datasets (i.e. observed and simulated) shows 12 nodes (Figure 6.4). SOMs classified the WERE based on the spatial patterns of southern African rainfall on WERE days. A close examination of the nodes, however, suggests that they can be broadly categorized into four different groups. The first group (i.e. nodes 1,5 and 9; hereafter TRW) shows nodes where rainfall occurs in a band starting from the tropics extending down towards the east coast. The pattern is most distint in node (1). The TRW WEREs account for 27.9% of the WEREs in the combined dataset, with node (1) WERE contributing the highest percentage (13%) in the group and the highest percentage of all the WEREs. However, Figure (6.5) shows that TRW WEREs are not seen often in the observational datasets (GPCP and TRMM). For instance, node (1) WEREs occurs twice in GPCP and TRMM, while the WEREs of the other two nodes are absent in observation. On the other hand, ERAINT and ARPEGE simulate the highest frequency (i.e. five events) of node (1) WEREs, while WRF simulates the highest occurrence (i.e. five events) of node (9). In general, most of the RCMs (except CCLM) simulate more TRW WEREs than observed. A further analysis of ERAINT composite data for TRW WERE days (Figures 6.6-6.8 and Table 6.1) suggests that TRW events are associated with events which are influenced by tropical troughs, angolan lows and ridging anticyclones, and therefore, some of these days could represent truncated Tropical Temperate Troughs (TTTs). The main moisture source on TRW WERE is the Indian Ocean, with some moisture coming from Mozambique due to evapotranspiration. The TRW WEREs occur in ERAINT during December, January, February and November. This makes sense since this group shows evidence of tropical systems which are prevalent during summer and rarely occur between the months of April and October (Tyson &Preston-Whyte, 2000; Todd & Washington, 1999). Most of the RCMs show that these WERE days occur during the months December-March. However, there are cases where they occur during the months April-October in the RCMs. In consistency with Kalognomou et al. (2013), WRF grossly overestimates the occurrence of TRW WEREs. Kalognomou et al. (2013) found that WRF overestimates precipitation over southern Africa in the summer months due to the model simulating higher intensity low pressure systems over the land as well as high moisture transport from the tropics and the Mozambique Channel. Since this group is associated with

low pressures over the continent as well as moisture transport from the Mozambique channel, one can see why WRF oversimulates these extreme events. Kalognomou et al. (2013) also states that WRF, REMO, PRECIS and ARPEGE tend to simulate stronger onshore flow over the south eastern parts of southern Africa all of these RCMs simulate higher WEREs associated with this group than the observed and with the exception of REMO, they all simulate higher frequencies of TRW WEREs than ERAINT.

The second group (nodes 6, 7 and 8; heareafter MLW) shows predominantly frontal like rain bands with the highest precipitation values occurring over the EC and further over the ocean within the frontal band. The nodes of this group combined contribute 21% of all the WERE days. TRMM only shows one WERE associated with this group, in node (7). GPCP on the other hand shows four WEREs (two in node 6 and two in node 8). ERAINT simulates the highest number of WEREs (i.e. four events) in node (6), and in node (7). CRCM5 and ERAINT simulate the highest occurrence of WEREs (i.e. three events). Other than CRCM5, most of the RCMs simulate the number of events associated with each node within the observed uncertainty. Analysing ERAINT composite data suggests that MLW WERE days occur over the EC when there is a mid-latitude cyclone over the region or just to the south-east of the region. These mid-latitude cyclones are seen, along with sub-tropical troughs, over the east coast and ridging anticyclones. The ERAINT composite data for each of these nodes still shows some tropical waves to the north of southern Africa, but the moisture flux doesn't show the transport of moisture from the north of southern Africa to the south east. Instead the moisture flux shows moisture either coming from the equatorial Indian ocean and then down into the east coast from Mozambique or from the Indian Ocean to the east or south of the east coast region. The ERAINT data shows that these synoptic conditions generally occur in the months December, September, October and March-May which suggests that mostly this group is associated with the shoulder season months. Most of the RCMs simulate the number of days overall and for each node within the observed uncertainty. CRCM5 simulates slightly higher values overall for the MLW group but the number of days associated with this group is not as high as those seen in ERAINT. Therefore, overall, downscaling ERAINT with the RCMs improves the simulations of the frequency of this type of rainfall pattern. Kalognomou et al. (2013) states that, during the

shoulder seasons, CORDEX errors are more influenced by the forcing boundary conditions than the internal physics and, perhaps, this is why we generally see better results for this group than the previous two.

The third group (i.e. nodes 10, 11 and 12; hereafter TMW) features WERE days that show frontal rain bands extending from the EC region further south east over the ocean. In these nodes, the frontal band is also connected by another band of rain to the more tropical regions of southern Africa. In the TMW nodes, the highest rainfall can be seen close to the east coast and over areas of high topography as well as over the ocean within the frontal rainband. The TMW nodes account for 22.1% of the WERE days in the combined datasets, with node (12) contributing 10%. TRMM shows no WEREs associated with the TMW nodes. GPCP on the other hand shows four WERE days associated with node (11) and none for the other TMW nodes. In node (11), GPCP shows the highest numbers of WEREs and all of the RCMs simulate WERE numbers within the observed uncertainty for this node. ERAINT, PRECIS and REGCM3 simulate the highest WEREs (i.e. three events) associated with node (10), while PRECIS and WRF simulate the highest WEREs (i.e. six and four events, respectively) for node (12). Therefore, downscaling ERAINT with WRF and PRECIS does not improve the simulation TMW WERE frequencies. ERAINT composite data for the WERE days (Figures 6.6-6.8 and Table 6.1) suggests that TMW events are associated with tropical troughs over the north of South Africa and mid-latitude cyclones and a ridging anticyclone further south. High MFC and moisture flux shows moisture being brought into the the north of southern Africa and down towards the east coast of South Africa. This kind of moisture transport is typical of a TTT (Van den Heever et al., 1997) which suggests that this group may represent events like TTTs, where tropical and mid-latitude synoptic conditions occur and interact. The ridging anticyclone also contributes to the moisture over the east coast region as it results in onshore flow of moisture from the ocean to the south or east of South Africa. In fact, this synoptic feature is mentioned by Hart et al. (2010) as one of the features present during a TTT, along with the northward extension of the SIA which can also be seen in the ERAINT nodes of this group. The particularly higher precipitation values, seen over the EC, are probably as a result of the ridging anticyclone and the steep topography intensifying the rainfall over this region (Hart et al., 2010). Again it is clear that WRF rainfall is sensitive to

tropical synoptic conditions and PRECIS seems sensitive to tropical and mid-latitude interactions. Along with WRF, Kalognomou et al. (2013) also found that PRECIS simulates higher intensity low pressures over the continent which may explain why these RCMs overestimate WEREs associated with this group.

The fourth group (nodes 2, 3 and 4; heareafter ISW) consists of nodes with very little rainfall over the tropics and less rainfall occurring over the ocean than seen in the TMW and MLW groups. Thus the rainfall for this group looks more isolated. The nodes in this group combined represent 27.7% of the total WERE days. TRMM shows that one of its three WERE days is associated with this group. This day is mapped to node (3) and the other nodes in the group are not associated with any TRMM WERE days. GPCP associates eight days with this group (two in node 2, three in node 3 and three in node 4). ERAINT shows the same amount of WERE days mapped to nodes (2) and (3) as GPCP and slightly more than GPCP (i.e. four events) mapped to node (4). Most of the RCMs simulate numbers of days inbetween the two observed datasets except for ARPEGE, who shows higher numbers in node (2) and node (4) (three and five days, respectively), and PRECIS, which shows the same number of days associated with node (2) as ARPEGE. The ERAINT data suggests that this group is associated with cut-off lows (nodes 2 and 3) or very steep westerly troughs (node 4) in the mid-troposphere; ridging anticyclones with a ridge over the east coast region; a subtropical trough over the east coast (nodes 3 and 4) or a west coast trough (node 2) . All the nodes show some presence of weak tropical waves but these seem disconnected from the sub-tropical and mid-latitude systems. The main moisture source for these conditions is the Indian Ocean, with moisture coming from north of Madagascar flowing over Mozambique and then south to the EC, with evapotranspiration over Mozambique possibly adding to the moisture received. Moisture is also transported from the Indian ocean to the south and east of the EC via the ridging anticyclone. According to ERAINT composite data, this group generally occurs in the months August to November. Tyson and Preston-Whyte (2000) state that the frequency of cut-off lows occur in March to May and September to November. Nodes (2) and (3) only show events occuring between September and November, which match what the authors stated. Node (4) shows an event in August and it is clear that node (4) shows the influence of mid-latitude cyclones as well. Overall this group

makes up for 36% of ARPEGE's total WERE days, therefore showing that ARPEGE simulates more isolated kinds of rainfall patterns associated with extreme rainfall over the EC. GPCP shows that these events are the most common WERE-causing events as 46% of GPCP WERE days are contained in this group.

When comparing the spatial rainfall patterns associated with WEREs over EC and WC, some similarities can be seen. The EC and WC both show WEREs which are influenced by tropical systems, with rainfall bands stretching from the north down to the EC or WC (truncated TTT-like rainfall). Both regions of study also show the influence of mid-latitude cyclones where frontal rainbands are seen and lastly both show WERE events where more isolated rainfall occurs. Differences in the WERE patterns can also be seen, in that EC shows TTT-like rainfall patterns whereas this is not seen for the WC. The WC also shows two distinct types of rainfall associated with mid-latitude cyclones in which higher rainfall is seen over the core of the Agulhas current in the one type and not the other. This distinction is not present over the EC, where high rainfall over the ocean is seen in all of the mid-latitude cyclone patterns.

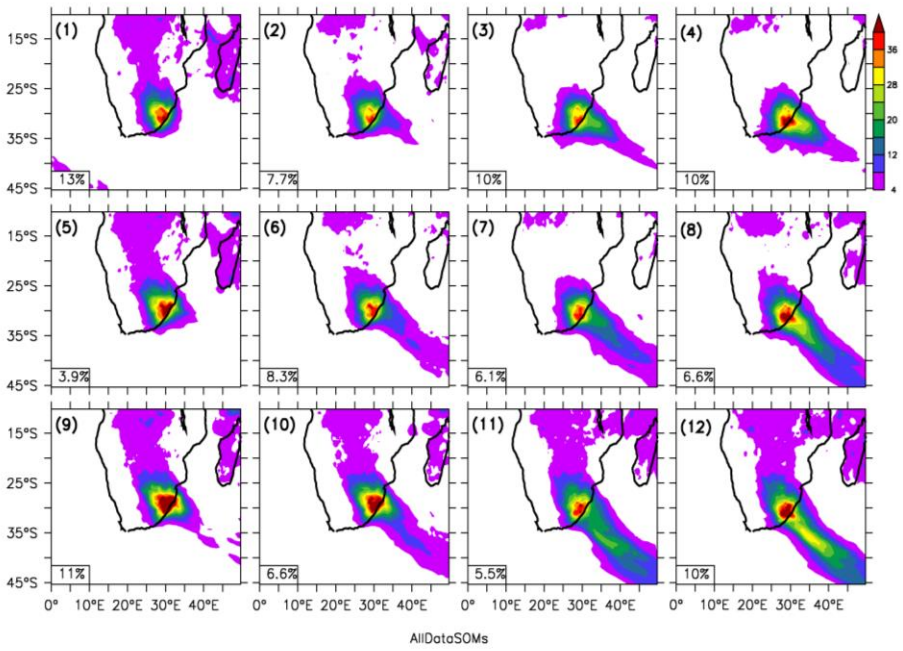

Figure 6.4: The SOMs classification (nodes) of widespread extreme rainfall events over the east coast region (1998-2008), obtained using both observed and simulated datasets.

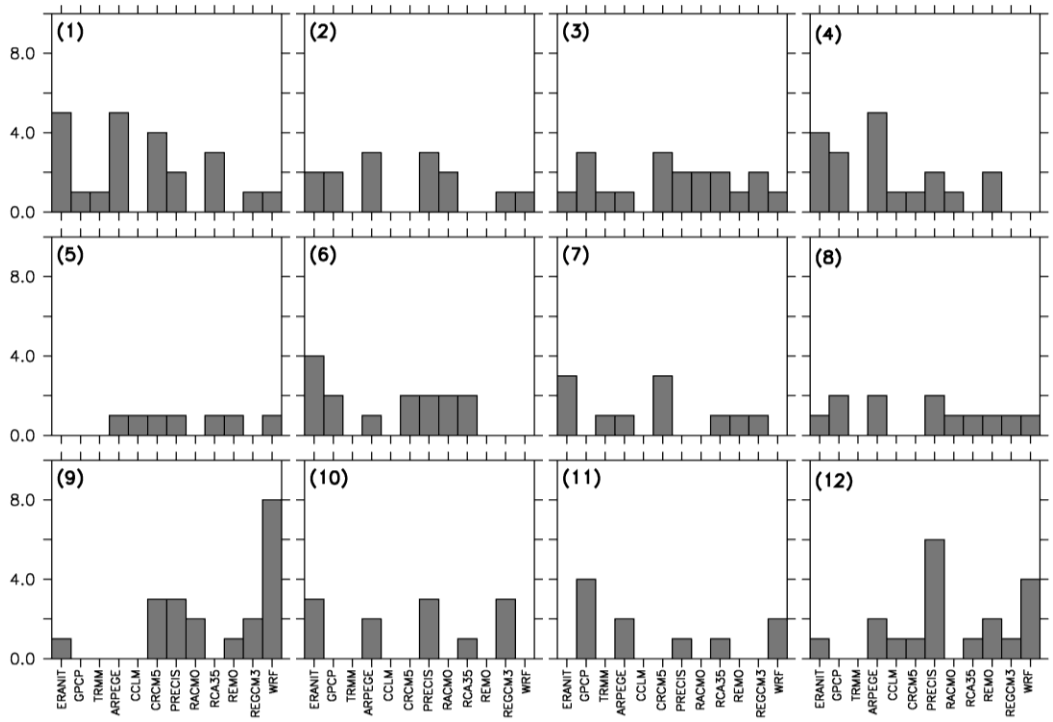

Figure 6.5: The frequency of the SOMs nodes (shown in Fig. 6.4) in the observed (GPCP and TRMM) and in simulated (ERAINT and CORDEX RCMs) datasets.

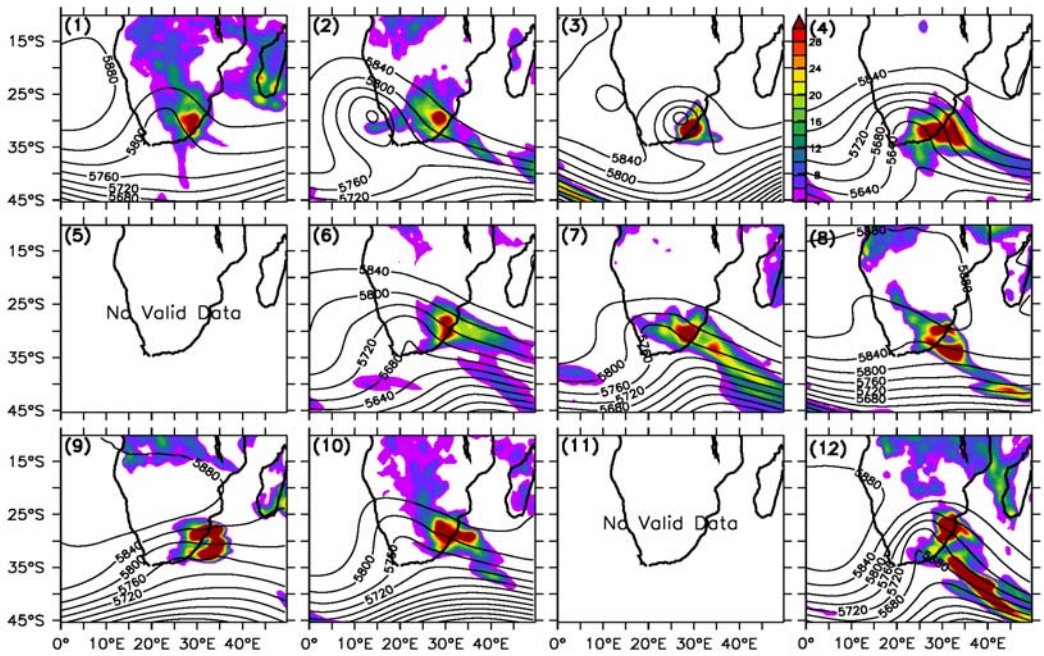

Figure 6.6: The composite of ERAINT rainfall contribution in the SOMs nodes (shown in Fig. 6.4) and the associated 500-mb geopotential heights.

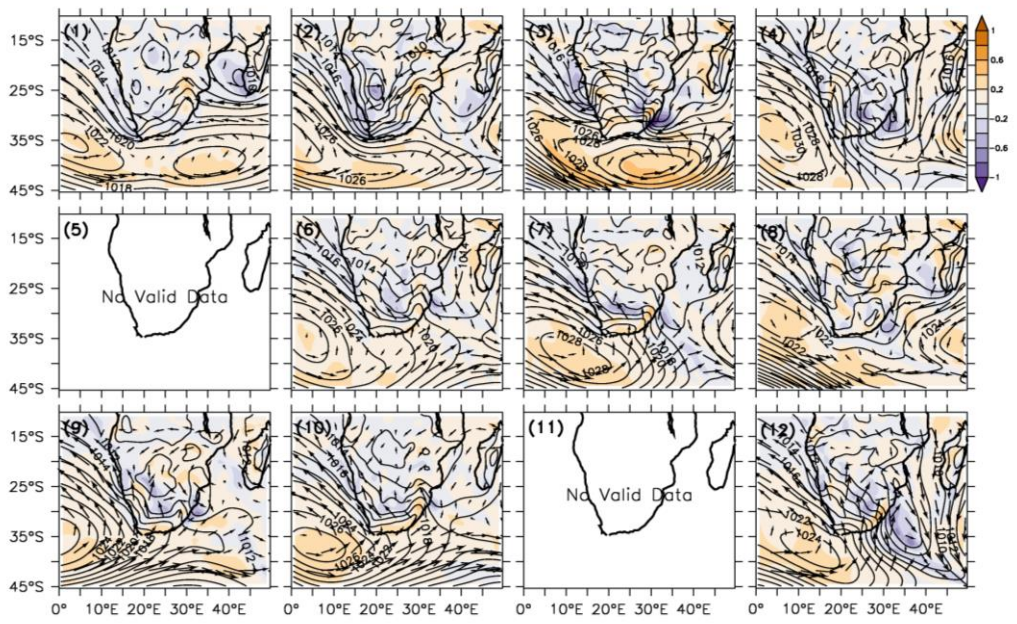

Figure 6.7: Same as Fig 6.6, but for the associated surface pressure (contour; mb) and 850 mb winds (arrows).

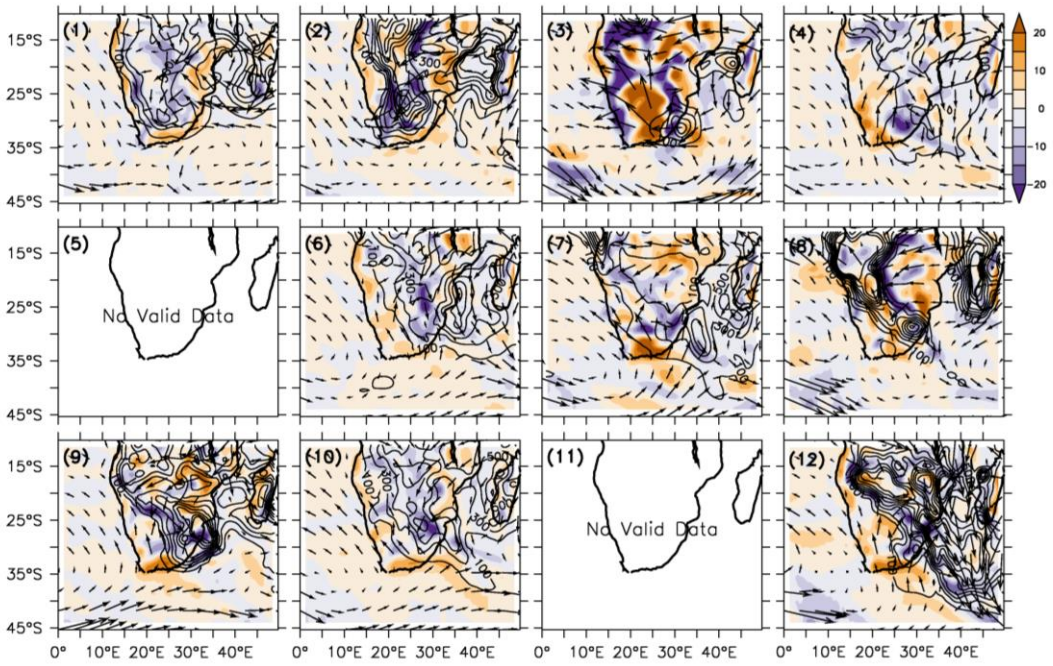

Figure 6.8: Same as Fig. (6.6), but for the associated CAPE (convective available potential energy (J/Kg), moisture fluxes (arrows) and moisture flux convergence (MFC; $\times\ 10^{-6}\mathrm{Kg}^2\mathrm{m}^2\mathrm{s}^{-2}$).

Table 6 1: Summary of Synoptic conditions seen for each node for Figures 6.6-6.8

Group	Node	Features
TRW	1	• At 500mb: weak westerly wave with a trough centered just west of the east coast region • At surface: Ridging anticyclone ridging over the east coast region, trough situated over the west of southern Africa , Angolan low and tropical trough • North Easterly 850hPa winds seen north of east coast region • Strong onshore flow over east coast region with cyclonic vorticity • High values of CAPE and Moisture Flux Convergence (MFC) over trough and west flank of ridging anticyclone and Moisture Flux Divergence (MFD) seen along the south and east coast of southern Africa • Strong moisture flux from the Indian Ocean off the east coast of South Africa
	9	• At 500mb: weak westerly wave (almost zonal) with a slight trough centered just west of the east coast region • At surface: Ridging anticyclone ridging across southern regions of South Africa, Angolan low and tropical trough • High values of CAPE and MFC all along the northern flank of the ridging anticyclone and MFD over south coast and northern east coast of southern Africa • Strong moisture flux from equatorial Indian Ocean
TMW	10	• At 500mb: steep westerly trough with axis centered over west coast of South Africa • At surface: Ridging anticyclone over east coast and mid-latitude cyclone further east and south of South Africa, Continental trough further north of the ridging anticyclone and tropical trough over west coast • Cyclonic vorticity on the west side of the ridging anticyclone • Higher values of CAPE and MFC seen along continental trough and northern regions of ridging high • Moisture flux from south Indian Ocean as well as equatorial Indian Ocean
	12	• At 500mb: steep westerly trough with axis centered just west of the east coast region • At surface: Mid-latitude cyclone over the east coast region between the South Indian Anticyclone (SIA) and the ridging South Atlantic Anticyclone (SAA) and a trough extending from 15°S down over the eastern regions of northern South Africa, tropical troughs seen over the west coast. • Cyclonic vorticity seen along the front and therefore over the northern region of the east coast • Onshore flow due to the ridging anticyclone seen in the southern

		regions of the east coast region • Very strong CAPE and MFC north of ridging anticyclone and along mid-latitude cyclone, MFD over south coast and western regions • Moisture flux from south Indian Ocean and the tropics
MLW	6	• At 500mb: westerly trough centered to the west of the east coast region. Trough not as steep as nodes (10) and (12) but steeper than node (1) and (9). • At surface: SAA ridging over the east coast region, mid-latitude cyclone seen further east of the coast, sub-tropical trough between Madagascar and east coast of South Africa, tropical troughs seen over the northern regions of southern Africa • Cyclonic vorticity seen on the westward side of the ridging anticyclone in the east coast region and along the mid-latitude cyclone • High Values of CAPE along sub-tropical trough, especially off the east coast • High Values of MFC seen along trough but especially on the west flank of the ridge over the east coast • Moisture flux from South Indian Ocean but strong moisture flux from tropical Indian Ocean.
	7	• At 500mb: Westerly Trough centered to the west of the east coast region. Trough not as steep as nodes (10) and (12) but steeper than node (1) and (9). • At surface: SAA ridging over the east coast region, mid-latitude cyclone, with associated east coast trough (sub-tropical trough), seen just off the east coast and tropical troughs seen over the northern west coast of southern Africa • Cyclonic vorticity seen above the western side of the ridging anticyclone and along the mid-latitude cyclone and east coast trough • High Values of CAPE and MFC above ridging anticyclone and along sub-tropical trough and MFD seen over south coast and over Mozambique • Moisture flux from tropical Indian Ocean and south Indian Ocean
	8	• At 500mb: very weak westerly trough with high pressure gradients over the south coast of South Africa • At surface: west coast trough, strong Angolan low, a mid-latitude cyclone, and its associated east coast trough, situated over the east coast region, tropical trough seen over west coast • Cyclonic vorticity seen over the east coast trough and along the mid-latitude cyclone. • Strong CAPE seen from the tropical trough down, over the Angolan low, to the east coast trough • Strong MFC seen along the east side of the Angolan low and west side of the subtropical east coast trough • Strong moisture flux from the equatorial Indian Ocean and some

		moisture also coming from the Indian Ocean just below Madagascar
ISW	2	• At 500mb: A cut-off low centered to the west of South Africa • At the surface: cut-off low subsumed in west coast trough, ridging anticyclone ridging over east coast region • Cyclonic vorticity seen along the southern areas of the east coast region which corresponds to the western flank of the ridging anticyclone and the eastern flank of the west coast trough • High CAPE and MFC along eastern side of west coast trough, MFD along west coast and east coast • Strong moisture flux from equatorial Indian ocean and slight moisture coming in from the Atlantic
	3	• At 500mb: A cut-off low with its center just slightly west of the east coast region • At the surface: Ridging anticyclone centered to the south of South Africa with a ridge over the east coast region, sub-tropical trough extending from Madagascar centered just off the east coast of South Africa, west coast trough extending from 15°S down to 30°S • Strong cyclonic flow seen over the sub-tropical trough and on the westward flank of the east coast region ridge • Strong CAPE values seen only over east coast region and in the Mozambique Channel, due to cut-off low and subtropical east coast trough. • Strong MFC over east coast • Moisture flux from Indian ocean just east of the east coast region
	4	• At 500mb: a very steep mid-latitude cyclone centered to the west of the east coast region • At the surface: an east coast trough extending across most of the sub-continent, a mid-latitude cyclone seen further south, with the SAA ridging behind it • Strong cyclonic flow seen over the east coast region • Highest Cape and MFC values seen over east coast and east coast trough • Moisture flux from the Agulhas current below the south coast

Chapter 7: Conclusion

This chapter provides the conclusions from the study, limitations of the study, and suggestions for future studies. The suggestions, which are based on the knowledge gained from the present study, will help overcome the limitations experienced in the present study and make the results of the study more robust and help to provide information on how to mitigate the impact of extreme rainfall events in South Africa.

7.1 Concluding remarks

As part of the efforts toward reducing the destructive impacts of extreme rainfall events in South Africa, this study has evaluated the capability of nine regional climate models in reproducing the characteristics of extreme rainfall events over South Africa, in particular, over the Western Cape and East Coast Areas. The nine RCMs (CCLM, REMO, PRECIS, CRCM5, ARPEGE, REGCM3, WRF, RACMO and RCA35) participated in the Coordinated Regional Climate Downscaling Experiment (CORDEX) and used ERA-Interim (ERAINT) as their boundary forcing. In the study we defined an extreme rainfall over a location as a rainfall that is equal or above the 95^{th} percentile of the rainfall distribution at the location, and defined widespread extreme rainfall events (WEREs) over an area as events during which more than 50% of the grid-points in the area experience extreme rainfall. We calculated the 95^{th} percentile threshold values over 11 years (1989-2008) of South Africa's daily rainfall data from the nine RCMS. The simulations were compared to two observation datasets (TRMM and GPCP), and to ERAINT rainfall data to understand whether these RCMs improve on the results from ERAINT. A self organizing map (SOM) was used to characterize WEREs identified in all the datasets into archetypal groups, and ERAINT data is used to describe the underlying circulations for each archetypal rainfall pattern. The number of WEREs mapped to each rainfall pattern for each dataset allows us to get an idea of whether certain RCMs are more likely to simulate certain rainfall patterns.

The correlation between the 95^{th} percentile threshold values of GPCP and the values of the RCMs, shows that, over South Africa, downscaling ERA-Interim (ERAINT) with CRCM5, RCA35, REMO and WRF improves the simulation of these values. However, regional biases need to be

taken into account as these models are not necessarily the best choice for the two regions of study. Over the east coast region (EC), the differences between the two observational datasets are larger than that over the Western Cape (WC). However, ERAINT simulates higher biases over the WC and these biases are seen in most of the RCMs as RACMO, REGCM3, REMO, WRF and CRCM5 show similar errors to ERAINT. When ERAINT is downscaled with ARPEGE, RCA35 and CCLM, the simulation of threshold values, over this region, improve, with CCLM showing the best results. Over the EC, the RCMs (CCLM, WRF and REMO) overestimate the threshold values, while two models (ARPEGE and REMO) show similar biases to ERAINT. Downscaling ERAINT with PRECIS seems to minimize the threshold value biases associated with this region. From the above, one can see that, while CCLM does well over the Western Cape it does poorly over the east coast region. ARPEGE does well over the Western Cape and produces similar results to ERAINT over the east coast region. This shows that some RCMs do well over certain regions and poorly over others. RCMs seem more sensitive to the ERAINT errors over the WC than EC, as more RCMs show errors similar to ERAINT over the Western Cape than the east coast region. This suggests that boundary-forcing data should also be chosen according to the region of study.

Some of the errors seen in the simulation of the threshold values over the two focus regions can be explained by looking at the rainfall distribution and cumulative rainfall distribution of each dataset over these two regions. Over both regions TRMM shows more frequent intense rainfall than GPCP. However, over the WC the observational uncertainty of the cumulative frequency distribution is less than that of the east coast region which may explain why differences in threshold values are higher over the EC. Over the EC, CCLM, WRF, REMO and PRECIS show much higher frequencies for intense rainfall which explains why CCLM, WRF and REMO overestimate the threshold values over this region. PRECIS, on the other hand, does not simulate high threshold values but still shows high frequencies of intense rainfall which can be explained by its over-simulation of widespread extreme rainfall events (WEREs). Over both the EC and the WC, CCLM simulates more intense rainfall than the other datasets. Over the EC, ERAINT simulates the lowest frequencies whereas over the WC, GPCP shows the lowest values.

When ERAINT is downscaled, using any of the RCMs, an enhanced frequency of intense rainfall over both the EC and the WC is simulated.

The number of widespread extreme rainfall events (WEREs) in each dataset provides some insight into which datasets show more grid scale extreme rainfall events and which show more synoptic scale extreme rainfall events. For both areas, GPCP observes a much larger amount of WEREs than TRMM, and ERAINT simulates more than both observed datasets, (although ERAINT simulates closer values to GPCP over the WC than the EC). Both the observed and reanalysis datasets show a higher amount of WERE days over the WC than the EC which may be owing to the fact that the WC contains a smaller amount of grid-points. Over both regions, downscaling ERAINT with CCLM results in the same amount of WEREs as TRMM. Downscaling ERAINT with PRECIS results in the simulation of the highest amount of WEREs compared to all the datasets. Whilst downscaling ERAINT with ARPEGE results in similar WERE numbers to ERAINT itself. Overall for both regions, it is very hard to conclude on the ability of the RCMs in simulating the monthly and annual frequency of WEREs as the observational differences are too large and the number of WERE events are not sufficient. Therefore using a longer time period and more observational datasets may provide more conclusive results.

The spatial characteristics of the precipitation of WEREs provides some insight into which areas are affected by what synoptic conditions which allows us to understand what conditions the RCMs might be sensitive to when simulating WEREs. Over both regions WERE events are induced by tropical systems where rainfall occurs over the northern regions of southern Africa and extends further south to the EC or WC. The EC and WC WEREs also show frontal rainfall patterns, induced by mid-latitude cyclones, as well as more isolated rainfall patterns. Over the EC, Tropical Temperate Trough (TTT)-like rainfall patterns can be seen, which is not prevalent in the WEREs over WC. The WC also shows two different groups of mid-latitude cyclone rainfall patterns—the one shows higher rainfall over the Agulhas current than the other. This is not the case for the EC where only one type of mid-latitude cyclone rainfall pattern is seen. For both the EC and the WC, the frequency of WEREs with rainfall caused by tropical systems, is generally overestimated by PRECIS. Over the EC, these types of WEREs are also overestimated

by WRF yet over the WC this is not the case. This suggests that the WRF WEREs are more sensitive to tropical systems over the EC than the WC. Over the EC, downscaling ERAINT with ARPEGE resulted in the over-simulation of isolated rainfall WEREs, whereas over the WC, WRF and CRCM5 underestimated the frequencies of these events. Over the EC, the MLW WEREs are better simulated than the tropical and isolated rainfall patterns, whereas over the WC this is not true.

7.2 Suggestions for further study

Further investigations are suggested to improve the understanding of the capabilities of RCMs, with an emphasis on CORDEX RCMs, in simulating extreme rainfall events over South Africa:

- In this study we used two observational datasets with a time period of 1998-2008. Investigating how the RCMs' simulation of extreme rainfall events compare to other observed datasets with longer time periods will help to further quantify the biases associated with the RCMs. This will be especially useful in looking at the frequency of extreme rainfall events where discrepancies in the observed datasets and the short time period made it difficult to find anything conclusive in this study.
- For this study we only used rainfall data from the RCM simulations but now more data from the CORDEX RCMs is being made available. With this in mind, further studies can be made in using this new data to investigate the atmospheric circulations simulated for extreme rainfall events in the RCMs which will help to further explain why certain models seem to simulate more extreme rainfall events during certain synoptic conditions.
- As concluded ERAINT seemed to influence the RCMs, in terms of the biases seen, more over the WC than the EC. Using different boundary conditions to force the RCMs may help to investigate whether this region is just more susceptible to the boundary conditions or whether it is ERAINT itself which results in higher biases over the region.
- Using different boundary conditions to force the RCMs can also help to elucidate whether the boundary conditions affect the synoptic conditions that the RCMs are sensitive to or whether these sensitivities are inherent to the RCM itself.

References

Bader, D., Covey, C., Gutowski, W., Held, I., Kunkel, K., Miller, R., & Zhang, M. (2008). Climate models: an assessment of strengths and limitations. *US Department of Energy Publications*, 8.

Barnston, A. G., & Mason, S. J. (2011).Evaluation of IRI's Seasonal Climate Forecasts for the Extreme 15% Tails. *Weather & Forecasting*, *26*(4).

Blamey, R. C., & Reason, C. J. C. (2012).Mesoscale Convective Complexes over Southern Africa. *Journal of Climate*, *25*(2). 1-53.

Brown, S. J., Caesar, J., & Ferro, C. A. (2008). Global changes in extreme daily temperature since 1950. *Journal of Geophysical Research: Atmospheres (1984–2012)*, *113*(D5).

Crimp, S. J., & Mason, S. J. (1999).The extreme precipitation event of 11 to 16 February 1996 over South Africa. *Meteorology and Atmospheric Physics*, *70*(1-2), 29-42.

Davis, C. L. (2011). Climate risk and vulnerability: a handbook for Southern Africa. *Council for Scientific and Industrial Research, Pretoria, South Africa*, *25*.

Dee, D. P., Uppala, S. M., Simmons, A. J., Berrisford, P., Poli, P., Kobayashi, S., &Vitart, F. (2011). The ERA-Interim reanalysis: Configuration and performance of the data assimilation system. *Quarterly Journal of the Royal Meteorological Society*, *137*(656), 553-597.

Denis, B., Laprise, R., Caya, D., &Côté, J. (2002). Downscaling ability of one-way nested regional climate models: the Big-Brother Experiment. *Climate Dynamics*, *18*(8), 627-646.

Dyson, L. L. (2009). Heavy daily-rainfall characteristics over the Gauteng Province. *Water SA*, *35*(5),627-638

Dyson, L. L., & Van Heerden, J. (2004).A model for the identification of tropical weather systems over South Africa. *Water SA*, *28*(3), 249-258.

Engelbrecht, C. J., Engelbrecht, F. A., & Dyson, L. L. (2013). High-resolution model-projected changes in mid-tropospheric closed-lows and extreme rainfall events over southern Africa. *International Journal of Climatology*, *33*(1), 173-187.

Engelbrecht, C., &Landman, W. A. (2013).Ridging highs 'out-rain'cut-off lows along the Cape South Coast. *ACCESS*, 7.

Giorgi, F., Jones, C., &Asrar, G. R. (2009). Addressing climate information needs at the regional level: the CORDEX framework. *World Meteorological Organization (WMO) Bulletin*, *58*(3), 175.

Goswami, B. N., Venugopal, V., Sengupta, D., Madhusoodanan, M. S., & Xavier, P. K. (2006). Increasing trend of extreme rain events over India in a warming environment. *Science*, *314*(5804), 1442-1445.

Grimm, A. M., &Tedeschi, R. G. (2009).ENSO and extreme rainfall events in South America. *Journal of Climate*, *22*(7), 1589-1609

Groisman, P. Y., Knight, R. W., & Karl, T. R. (2001). Heavy precipitation and high streamflow in the contiguous United States: Trends in the twentieth century. *Bulletin of the American Meteorological Society*, *82*(2), 219-246.

Hart, N. C. G., Reason, C. J. C., &Fauchereau, N. (2010). Tropical–Extratropical Interactions over Southern Africa: Three Cases of Heavy Summer Season Rainfall. *Monthly Weather Review*, *138*(7).

Hewitson, B. C., & Crane, R. G. (2002). Self-organizing maps: applications to synoptic climatology. *Climate Research*, *22*(1), 13-26.

Holloway, A., Fortune, G., Chasi, V., Beckman, T., & Disaster Mitigation for Sustainable Livelihoods Programme (University of Cape Town). (2010). *RADAR Western Cape 2010: Risk and development annual review*. Rondebosch: PeriPeri Publications.

Hudson, D. A., & Jones, R. G. (2002). Regional climate model simulations of present-day and future climates of southern Africa. *Hadley Centre Technical Note*, *39*, 41.

Huffman, G. J., Adler, R. F., Bolvin, D. T., Gu, G., Nelkin, E. J., Bowman, K. P., Hong, Y., Stocker E. F., & Wolff, D. B. (2007). The TRMM Multisatellite Precipitation Analysis (TMPA): Quasi-global, multiyear, combined-sensor precipitation estimates at fine scales. *Journal of Hydrometeorology*, *8*(1).

Huffman, G. J., Adler, R. F., Morrissey, M. M., Bolvin, D. T., Curtis, S., Joyce, R., McGavock , B. & Susskind, J. (2001). Global precipitation at one-degree daily resolution from multisatellite observations. *Journal of Hydrometeorology*, *2*(1), 36-50.

Intergovernmental PanelOn Climate Change. (2001). *Climate change 2001 IPCC third assessment report*. Geneva, IPCC Secretariat.

Iseri, Y., Matsuura, T., Iizuka, S., Nishiyama, K., & Jinno, K. (2009). Comparison of pattern extraction capability between self-organizing maps and principal component analysis. *Memoirs of the Faculty of Engineering, Kyushu University*, *69*(2), 37-47.

Jacob, D., Petersen, J., Eggert, B., Alias, A., Christensen, O. B., Bouwer, L. M., & Yiou, P. (2013). EURO-CORDEX: new high-resolution climate change projections for European impact research. *Regional Environmental Change*, 1-16.

Kalognomou, E. A., Lennard, C., Shongwe, M., Pinto, I., Favre, A., Kent, M., & Büchner, M. (2013). A Diagnostic Evaluation of Precipitation in CORDEX Models over Southern Africa. *Journal of Climate*, *26*(23).

Kim, J., Waliser, D. E., Mattmann, C. A., Goodale, C. E., Hart, A. F., Zimdars, P. A., & Favre, A. (2013). Evaluation of the CORDEX-Africa multi-RCM hindcast: systematic model errors. *Climate Dynamics*, 1-14.

Klein Tank, A. M. G., & Zwiers, F. W. (2009). Guidlines on Analysis of Extremes in a Changing Climate in Support of Informed Decisions for Adaptation. *Climate Data and Monitoring, 72* . World Meteorological Organisation .

Kohonen, T. (1990).The self-organizing map. *Proceedings of the IEEE*, *78*(9), 1464-1480.

Landman, W. A., &Beraki, A. (2012). Multi-model forecast skill for mid-summer rainfall over southern Africa. *International Journal of Climatology*, *32*(2), 303-314.

Landman, W. A., & Goddard, L. (2002). Statistical recalibration of GCM forecasts over southern Africa using model output statistics. *Journal of Climate*,*15*(15).

Landman, W. A., Botes, S., Goddard, L., &Shongwe, M. (2005).Assessing the predictability of extreme rainfall seasons over southern Africa. *Geophysical research letters*, *32*(23).

Lennard, C. J., Coop, L., Morison, D., & Grandin, R. (2013). *Extreme Events: Past and future Changes in the Attributes of Extreme Rainfall and the Dynamics of their Driving Processes.* Water Research Commission.

Liu, Yonggang, Robert H. Wesiberg, and Ruoying He. "Sea surface temperature patterns on the West Florida Shelf using growing hierarchical self-organizing maps." *Journal of Atmospheric and Oceanic Technology* 23 (2006): 325-338.

Mason, S. J., &Joubert, A. M. (1997).Simulated changes in extreme rainfall over southern Africa. *International journal of climatology*, *17*(3), 291-301.

Mason, S. J., Waylen, P. R., Mimmack, G. M., Rajaratnam, B., & Harrison, J. M. (1999).Changes in extreme rainfall events in South Africa. *Climatic Change*,*41*(2), 249-257.

Mélice, J. L., & Reason, C. J. (2007). Return period of extreme rainfall at George, South Africa. *South African Journal of science*, *103*(11-12), 499-501.

Murshed, M. S., Kim, S., & Park, J. S. (2011).Beta-κ distribution and its application to hydrologic events. *Stochastic Environmental Research and Risk Assessment*, *25*(7), 897-911.

Nikulin, G., Jones, C., Giorgi, F., Asrar, G., Büchner, M., Cerezo-Mota, R. & Sushama, L. (2012). Precipitation Climatology in an Ensemble of CORDEX-Africa Regional Climate Simulations. *Journal of Climate*, *25*(18).

Rajczak, J., Pall, P., &Schär, C. (2013).Projections of extreme precipitation events in regional climate simulations for Europe and the Alpine Region. *Journal of Geophysical Research: Atmospheres*, *118*(9), 3610-3626.

Reason, C. J. C., Landman, W., & Tennant, W. (2006).Seasonal to decadal prediction of southern African climate and its links with variability of the Atlantic Ocean. *Bulletin of the American Meteorological Society*, *87*(7).

Rouault, M., Jobard, I., White, S. A., &Lutjeharms, J. R. E. (2001). Studying rainfall events over South Africa and adjacent oceans using the TRMM satellite: research in action. *South African journal of science*, *97*(11 & 12), p-455.

Rouault, M., White, S. A., Reason, C. J. C., Lutjeharms, J. R. E., &Jobard, I. (2002). Ocean–Atmosphere Interaction in the Agulhas Current Region and a South African Extreme Weather Event. *Weather & Forecasting*, *17*(4), 655-669.

Sanderson, M. (2010).Changes in the frequency of extreme rainfall events for selected towns and cities. *Ofwat, UK*.

Sen Roy, S., & Rouault, M. (2013).Spatial patterns of seasonal scale trends in extreme hourly precipitation in South Africa. *Applied Geography*, *39*, 151-157.

Shongwe, M. E., Van Oldenborgh, G. J., Van Den Hurk, B. J. J. M., De Boer, B., Coelho, C. A. S., & Van Aalst, M. K. (2009). Projected Changes in Mean and Extreme Precipitation in Africa under Global Warming. Part I: Southern Africa. *Journal of Climate*, *22*(13).

Singleton, A. T., & Reason, C. J. C. (2006). Numerical simulations of a severe rainfall event over the Eastern Cape coast of South Africa: sensitivity to sea surface temperature and topography. *Tellus A*, *58*(3), 355-367.

Singleton, A. T., & Reason, C. J. C. (2007).A Numerical Model Study of an Intense Cutoff Low Pressure System over South Africa. *Monthly weather review*,*135*(3).

Skupin, A., & Agarwal, P. (2008). Introduction: What is a Self-Organizing Map?.*Self-organising maps: Applications in geographic information science*, 1-20.

South African Weather Service (SAWS). 20011a. Climate Summary of South Africa, November 2011, 23(11).

South African Weather Service (SAWS). 2007. Climate Summary of South Africa, June 2007, 18(6).

South African Weather Service (SAWS). 2009. Climate Summary of South Africa, July 2009, 20(7).

South African Weather Service (SAWS). 2011b. Climate Summary of South Africa, June 2011, 22(6).

South African Weather Service (SAWS). 2011c. Climate Summary of South Africa, January 2011, 23(1).

South African Weather Service (SAWS). 2012. Climate Summary of South Africa, July 2012, 23(7).

Sylla, M. B., Giorgi, F., Coppola, E., &Mariotti, L. (2013). Uncertainties in daily rainfall over Africa: assessment of gridded observation products and evaluation of a regional climate model simulation. *International Journal of Climatology*,*33*(7), 1805-1817.

Taljaard, J. J. (1996). Atmospheric Circulation Systerms, Synoptic Climatology and Weather Phenomena of South Africa Part 6: Rainfall in South Africa. *Weather Bureau Technical Paper, 32*.

Todd, M., & Washington, R. (1999). Circulation anomalies associated with tropical-temperate troughs in southern Africa and the south west Indian Ocean.*Climate Dynamics*, *15*(12), 937-951.

Tošić, I., &Unkašević, M. (2013).Extreme daily precipitation in Belgrade and their links with the prevailing directions of the air trajectories. *Theoretical and applied climatology*, *111*(1-2), 97-107.

Tyson, P. D., & Preston-Whyte, R. A. (2000). *Weather and climate of southern Africa*. Cape Town: Oxford University Press.

Van den Heever, S. C., D'Abreton, P. C., & Tyson, P. D. (1997).Numerical simulation of tropical-temperate troughs over southern Africa using the CSU RAMS model.

Williams, C. J. R., Kniveton, D. R., &Layberry, R. (2008). Influence of South Atlantic Sea Surface Temperatures on Rainfall Variability and Extremes over Southern Africa. *Journal of Climate*, *21*(24), 6498-6520.

Williams, C. J. R., Kniveton, D. R., &Layberry, R. (2010). Assessment of a climate model to reproduce rainfall variability and extremes over Southern Africa. *Theoretical and applied climatology*, *99*(1-2), 9-27.

Williams, C. J., Kniveton, D. R., &Layberry, R. (2011). Extreme Rainfall Events over Southern Africa. In *African Climate and Climate Change* (pp. 71-100). Springer Netherlands.

Zhang, Q., Körnich, H., & Holmgren, K. (2013). How well do reanalyses represent the southern African precipitation?. *Climate dynamics*, *40*(3-4), 951-962.

Zhang, Q., Körnich, H., & Holmgren, K. (2013). How well do reanalyses represent the southern African precipitation?. *Climate dynamics*, *40*(3-4), 951-962.